Available online at www.sciencedirect.com
SCIENCE DIRECT®
PERGAMON
Organic Geochemistry 34 (2003) 1651–1672
Organic Geochemistry
www.elsevier.com/locate/orggeochem

Insights into oil cracking based on laboratory experiments☆

Ronald J. Hill[a,*], Yongchun Tang[b], Isaac R. Kaplan[c]

[a]United States Geological Survey, DFC, Box 25046, M.S. 939, Denver, CO 80225, USA
[b]California Institute of Technology, Pasadena, CA 91789, USA
[c]Department of Earth and Space Science and IGPP, University of California, Los Angeles, CA 80401, USA

Received 19 November 2002; accepted 24 July 2003
(returned to author for revision 1 March 2003)

Abstract

The objectives of this pyrolysis investigation were to determine changes in (1) oil composition, (2) gas composition and (3) gas carbon isotope ratios and to compare these results with hydrocarbons in reservoirs. Laboratory cracking of a saturate-rich Devonian oil by confined, dry pyrolysis was performed at $T=350$–450 °C, $P=650$ bars and times ranging from 24 h to 33 days. Increasing thermal stress results in the C_{15+} hydrocarbon fraction cracking to form C_{6-14} and C_{1-5} hydrocarbons and pyrobitumen. The C_{6-14} fraction continues to crack to C_{1-5} gases plus pyrobitumen at higher temperatures and prolonged heating time and the $\delta\ ^{13}C_{ethane}$–$\delta^{13}C_{propane}$ difference becomes greater as oil cracking progresses. There is considerable overlap in product generation and product cracking. Oil cracking products accumulate either because the rate of generation of any product is greater than the rate of removal by cracking of that product or because the product is a stable end member under the experimental conditions. Oil cracking products decrease when the amount of product generated from a reactant is less than the amount of product cracked. If pyrolysis gas compositions are representative of gases generated from oil cracking in nature, then understanding the processes that alter natural gas composition is critical.

1. Introduction

Oil cracking involves the redistribution of hydrogen from precursor oil to the more thermodynamically stable products of methane in the hydrogen-rich gas phase and pyrobitumen in the carbon-rich solid phase (Takach et al., 1987). Numerous studies have been conducted to determine how oil composition changes with increases in thermal stress with an emphasis on the kinetics of oil cracking (Bjoroy et al., 1988; Ungerer et al., 1988; Behar et al., 1991, 1992; Horsfield et al., 1992; Kuo and Michael, 1994; Pepper and Dodd, 1995; Schenk et al., 1997; Tsuzuki et al., 1999). Previous work established that as oil cracks, high molecular weight (HMW) hydrocarbons and heteroelement (N, S, O) compounds are transformed into progressively low molecular weight (LMW) compounds (condensate and gas) and pyrobitumen. Early work suggested oil was only stable to 150 °C (McNab et al., 1952) and there is still a perception that oil cannot be found at temperatures greater than 150 °C (Barker, 1990; Hayes, 1991). An increasing body of data, however, suggests that oil is stable to 200 °C. Field evidence (Price et al. 1979, Price, 1981; Price et al., 1981; Mango, 1990; Horsfield et al., 1992; Schenk et al., 1997), laboratory evidence (Domine, 1989, 1991; Domine and Enguehard, 1992; Horsfield et al., 1992; Price, 1995; Schenk et al., 1997) and theoretical calculations (Domine et al., 1990, 1998) all support oil stability to 200 °C.

Bjoroy et al. (1988) performed oil cracking experiments in stainless steel reactors at temperatures between 310 and 370 °C for durations of up to 8 days, in the

☆ Institute of Geophysics and Planetary Physics Publication No. 5761.

* Corresponding author. Tel.: +1-303-236-1534; fax: +1-303-236-0459.
E-mail address: ronhill@usgs.gov (R.J. Hill).

0146-6380/$ - see front matter © 2003 Elsevier Ltd. All rights reserved.
doi:10.1016/S0146-6380(03)00173-6

presence of water. No attempt was made to control pressure. They found that increasing temperature and time of pyrolysis resulted in greater cracking of C_{15+} components to C_{15-} hydrocarbons. They also found that branched and cyclic compounds reacted or cracked faster than *n*-alkanes and that the residual oil becomes more aromatic. Furthermore, they observed oil-like liquids generated from the NSO compounds fraction.

Ungerer et al. (1988) performed sealed gold tube pyrolysis experiments of oils at temperatures ranging from 335 to 540 °C and durations between 10 min and 14 days. Pyrolysis of two oils resulted in generation of $C_{1–13}$ hydrocarbons and pyrobitumen from cracking of the C_{14+} fraction. The C_{14+} residue was composed predominantly of polyaromatic compounds. Decomposition of the $C_{6–13}$ fraction resulted in generation of methane and $C_{2–5}$ with a predominance of aromatic compounds in the $C_{6–13}$ residue. The $C_{2–5}$ fraction ultimately decomposed into methane and pyrobitumen. The asphaltenes and resins decomposed early. Aromatic oils produced more pyrobitumen than paraffinic oils.

Behar et al. (1991, 1992) performed confined pyrolysis of kerogen and the oil-like pyrolysate generated from the kerogen at 365–540 °C, confinement pressure of 120 bars or less and durations ranging from a few minutes to 1 month. They conjectured that the oil-like C_{14+} fraction was derived from the cracking of kerogen and the generated asphaltene and resin fractions. The $C_{2–5}$ and $C_{6–13}$ fraction yields were highest during C_{14+} degradation and were mainly derived from oil cracking with minor amounts coming from kerogen cracking. Methane became the main gas generated after $C_{6–13}$ fraction degradation was complete. Aromatic compounds predominated in the $C_{6–13}$ and C_{14+} fractions as cracking of saturates in these fractions increased.

Horsfield et al. (1992) and Schenk et al. (1997) pyrolysed oils using the microscale sealed vessel (MSSV) technique at heating rates of 0.1, 0.7 and 5.0 °C/min. Internal pressure was estimated to be 30 bars or less. They found that the C_{15+} fraction begins to crack first, resulting in formation of $C_{1–5}$ and $C_{6–13}$ fractions. Asphaltene and resin cracking was postulated to start during C_{15+} cracking. The $C_{6–13}$ fraction cracked to wet gas and the wet gas ultimately cracked to methane and pyrobitumen. Pyrobitumen formation was suspected to start during asphaltene and resin cracking. Increased paraffinicity of the residual oil was noted before *n*-alkane cracking commenced. After *n*-alkane cracking was initiated, the residual oil became increasingly aromatic.

Pepper and Dodd (1995) conducted sealed platinum pyrolysis experiments to investigate oil cracking in the presence of residual source rock. They found the oil cracking process and derived kinetic parameters were highly dependent on the oil composition, with the saturated to aromatic hydrocarbon ratio of primary importance. They also acknowledged that the cracking of oil in reservoir may be very different than cracking in the presence of a source rock, where kerogen and minerals may act as hydrogen donors.

Previous studies have established that cracking of HMW compounds to LMW compounds is the dominant process during oil cracking and that pyrobitumen formation cannot be ignored. These studies, focused on the kinetics of oil cracking, also suggest that oil is stable at higher temperatures than previously recognized. In this study we investigated controls on the yield of C_{15+}, $C_{6–14}$, $C_{2–5}$, C_1 and pyrobitumen. NSO compound evolution and the contribution of NSO cracking products to oil has been addressed. We also investigate the progression of gas composition and the timing of pyrobitumen formation during pyrolysis with an emphasis on the implications for hydrocarbon cracking in reservoirs, natural gas composition and gas accumulation.

2. Methods

2.1. Pyrolysis

Sealed gold tube pyrolysis was performed at temperatures ranging from 350 to 450 °C at 650 bars pressure and times ranging from 1 to 33 days. Most experiments fall into the post oil generation stage of Lewan (1985). The gold tubing, bombs, furnaces, temperature control and pressure control systems, gold tube preparation, sample loading and experimental procedure used in the pyrolysis experiments are described in Hill et al. (1994, 1996) and are summarized briefly here. The gold tubing is cleaned and then annealed in a furnace at 950 °C for 12 h. One end of the gold tube is welded close and then approximately 50 μl of oil are pipetted into the gold tube. The gold tube containing the oil is then flushed with argon and the open end crimped with pliers, clipped to create a smooth welding surface and then welded closed. Weight of the gold tube plus oil sample is recorded before and after the experiment to assess the integrity of each experiment. The gold tubes were then placed in pressure vessels and the pressure vessels placed into furnaces. Water was used as the external pressure medium.

The starting material for the confined pyrolysis experiments was a 35° API gravity Devonian oil from the Western Canada Sedimentary Basin in Alberta, Canada. The whole oil stable carbon isotope ratio is −29.47‰ relative to PDB. The bulk composition of the oil, determined after topping the oil at 35 °C for 2.5 h under vacuum is 64% saturates, 23% aromatics, 7% resins and 7% asphaltenes. The oil falls into the Cynthia shale oil family of Allan and Creaney (1991).

2.2. Gas product analysis

After pyrolysis, the gold tube was placed in a piercing device and attached to a vacuum line equipped with a toepler pump, calibrated burette and plumbed to a gas chromatograph for hydrocarbon and non-hydrocarbon gas analysis. Gas collection was initiated by puncturing the gold tube under vacuum. The pyrolysate was initially exposed for 5 min to a removable dry ice/acetone bath ($T=-77$ °C) attached to the gold tube puncturing devise. The pyrolysate gas was then expanded into a liquid nitrogen trap ($T=-196$ °C) for 5 min. The liquid nitrogen non-condensable gases (N_2, CH_4, CO and H_2) were moved into the calibrated burette using a toepler pump. The gases were quantified by injection into a Untied Technologies gas chromatography as described by Hill et al. (1994, 1996). The liquid nitrogen condensable gases (CO_2, Ar, and C_{2-5} hydrocarbons) were then warmed to room temperature, pumped into the calibrated burette, frozen into a glass tube that was then sealed and analyzed by injection into a Hewlett Packard 5890 gas chromatography as described by Hill et al. (1994, 1996).

For duplicate runs of each experiment, stable carbon isotope ratio measurements on methane, ethane and propane were obtained. The gases were collected as described above and analyzed using the methods of Hill et al. (1994, 1996). Results are reported in δ notation relative to PDB standard and were calibrated assuming $\delta^{13}C(NBS\text{-}22)=-29.81‰$. The errors on isotope measurements are ±0.1‰ for methane and 0.2‰ for other gases.

2.3. Liquid product analysis

Following gas analysis, the punctured gold tube was removed from the puncturing device, cut open with clippers and the residual oil extracted three times by sonication in pentane to obtain the approximately C_{10+} residual saturate, aromatic and resin liquid fraction. Although extraction was carefully performed, evaporation of some hydrocarbons in the $C_{10–14}$ range almost certainly occurred. The pentane extract was decanted and passed through a 0.45 μm nylon filter to recover any pyrobitumen and asphaltenes. The trap that was attached to the puncturing device and contained the dry ice/acetone condensable material was removed and the trap rinsed three times with pentane to obtain the $\sim C_{6–12}$ fraction that was then added to the gold tube pentane extract. There is overlap in the compounds trapped by dry ice/acetone and the compounds extracted with pentane from the gold tube. When the two extracts are combined, a C_{6+} extract is obtained and analyzed by GC. The pentane extract was then diluted to 15–20 ml, 200 μl of pentane extract was then mixed with 200 μl of internal standard containing deuterated C_{16}, C_{20}, C_{24}, and C_{32}. Each compound in the standard solution was present in approximately 0.15 mg/ml concentrations (exact concentrations known). A portion of the pentane extract was evaporated and separated by high performance liquid chromatography (HPLC) to quantify the total saturated, total aromatic and resin fractions.

After extraction by pentane, the remaining oil cracking residue in the gold tube was extracted three times by sonication using dichloromethane. The dichloromethane extract was filtered through the same 0.45 μm nylon paper to collect additional pyrobitumen and to solublize any asphaltenes retained on the filter paper. In this step, any asphaltenes precipitated during pentane extraction and collected on the filter paper are solublized by the dichloromethane and collected as part of the dichloromethane extract. The filter paper was dried and weighed to determine the amount of pyrobitumen formed. The dichloromethane extracts were diluted to 10 ml and then 200 μl mixed with 200 μl of internal standard for quantification purposes. A portion of the dichloromethane extract was evaporated and used for quantification of resins and asphaltenes. The extraction procedures are summarized in Fig. 1.

The total weight of C_{15+} fraction was determined by combining data from the pentane and dichloromethane extraction steps. The extracts were not combined. The pentane and dichloromethane extracts were separately evaporated to constant weight to determine the C_{15+} fraction weight in each. The pentane extract was used to determine total weight of saturates + aromatics + resins. The dichloromethane extract was used to determine the weight of asphaltenes and any resins that may have precipitated with the asphaltenes.

The total weight of C_{15+} saturated hydrocarbon, aromatic hydrocarbon and resin compounds in the pentane extract were determined by HPLC separation. The weight of resins and asphaltenes in the dichloromethane extract were determined by precipitation and separation on a silica gel column. These results combined with the gas data were used to determine the total mass balance for each experiment. The concentration of total $C_{6–14}$, n-C_{15+} alkanes and total isoprenoids was determined by GC analysis.

The reproducibility of multiple gold tube experiments run at the same temperature (T), pressure (P) and time (t) conditions was 5% for methane and 6% for ethane, propane, the butanes, pentanes and CO_2. The gold tube extract reproducibility was 8% for saturate and aromatic C_{15+} components, 15% for NSOs, 11% for $C_{6–14}$ and 6% for pyrobitumen.

2.4. Data representation

We defined the oil precursor and pyrolysis products in terms of $C_{15+}C_{6–14}$, $C_{2–5}$, C_1, and pyrobitumen fractions (Fig. 2), similar to the products of Ungerer et al.

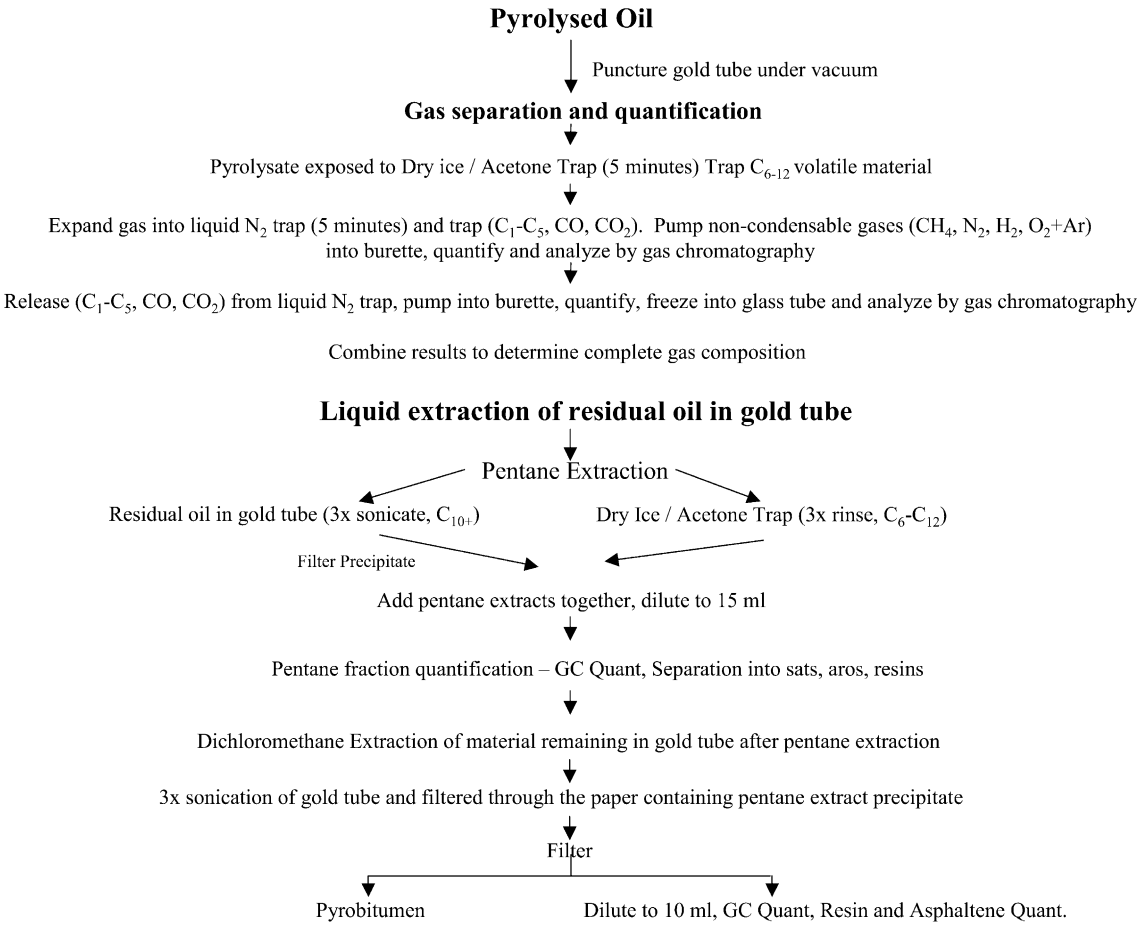

Fig. 1. Scheme for analysis of experimental products.

Oil Cracking Scheme

1. NSO $\longrightarrow C_{15+HC} + C_{6-14} + C_{2-5} + C_1$ + pyrobitumen
2. $C_{15+} \longrightarrow C_{6-14} + C_{2-5} + C_1$ + pyrobitumen
3. $C_{6-14} \longrightarrow C_{2-5} + C_1$ + pyrobitumen
4. $C_{2-5} \longrightarrow C_1$ + pyrobitumen

Fig. 2. Oil cracking scheme based on experimental observations.

(1988) and Behar et al. (1991, 1992). The C_{15+} fraction includes hydrocarbons plus NSO compounds. Changes in the NSO compound fraction are also discussed as these changes have implications for other trends observed in the experiments. The thermal maturity of the experiments is expressed as equivalent vitrinite reflectance (%R_o) calculated using the experimental times and temperatures and Easy R_o[1] (Sweeney and Burnham, 1990). The percent oil cracked is determined by adding the weight of $C_{1–5}$ gas and the weight of pyrobitumen generated and then dividing that total by the starting oil weight. There is a gap in experimental results between %R_o ~1.7–2.3 due to failure of long run time experiments (Fig. 3).

3. Results

3.1. C_{15+} (hydrocarbons plus NSO compounds)

The data collected from the pentane extractions and dichloromethane extraction steps were combined to determine mass balance and are summarized in Table 1. During pyrolysis, HMW C_{15+} compounds crack to form the LMW components $C_{6–14}$, $C_{2–5}$, C_1, non-hydrocarbon gases, and pyrobitumen with increasing thermal stress (pyrolysis time and temperature; Table 1 and Fig. 3). The C_{15+} yield decreases from a pre-pyrolysis value of 765 mg/g to about 150 mg/g at %R_o ~1.7 (360 °C, 33.3 days) and increases to ~220

[1] Any use of trade, product, or firm names is for descriptive use only and does not imply endorsement by the US government.

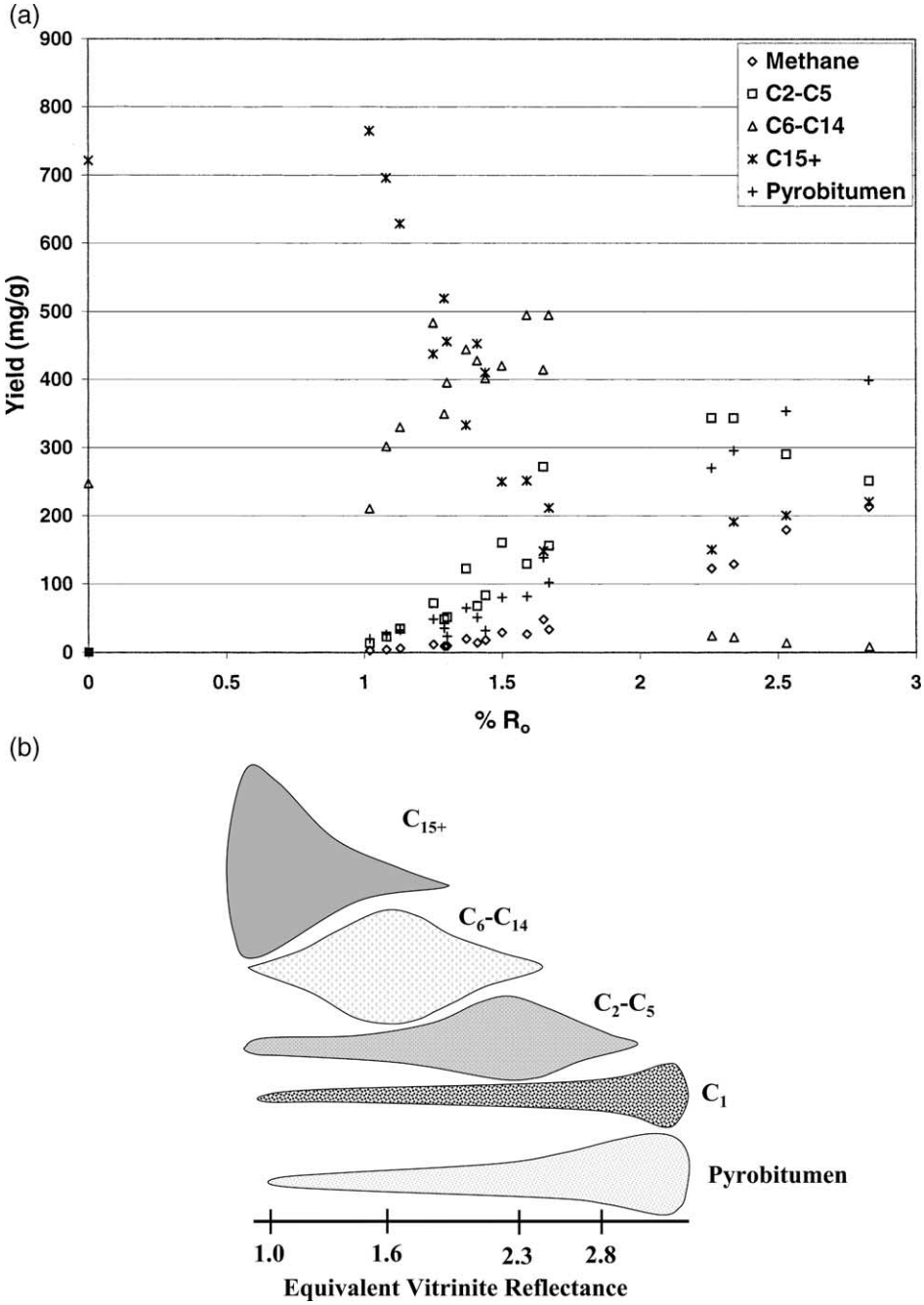

Fig. 3. (a) Changes in pseudo-component yield as a function of increasing thermal stress. Initially, $C_{6–14}$, $C_{2–5}$, C_1 and pyrobitumen are generated as C_{15+} is cracked. At higher $\%R_o$, $C_{6–14}$ cracking is predominant resulting in $C_{2–5}$, C_1 and pyrobitumen. Ultimately cracking of the $C_{2–5}$ fraction predominates. There is overlap in cracking reactions. Hydrocarbon fraction maxima are controlled by relative reaction rates and reactant supply. (b) Schematic diagram showing the overlap in generation and cracking of hydrocarbon products and pyrobitumen. $\%R_o$ values are calculated using Easy R_o and reflect experimental conditions.

Table 1
Changes in residual oil and cracked products during pyrolysis at various temperatures and lengths of time with pressure held constant at 650 bars

Sample ID	Devonian Oil	317	314	313	311	333	307	300	302	304	318	319	322	324	351	364	261	267
Temperature (°C)	Reference	350	350	350	350	360	360	360	360	360	370	380	390	400	440	450	450	450
Time (days)	–	3	4.3	12	20.3	3	6	12	24	33.3	3	3	3	3	3	1	3	6
Sample wt (mg)	45.9	47.44	47.71	50.18	49.36	45.45	47.74	46.34	46.37	47.86	48.17	47.47	53.24	47.51	49.74	45.53	45.27	47.14
Hydrogen (mg/g)		0.02	0.01	0.02	0.02	0.02	0.02	0.03	0.03	0.03	0.03	0.06	0.06	0.06	0.17	0.15	0.17	0.16
Carbon monoxide (mg/g)	<0.01	<0.01	<0.01	<0.01	<0.01	<0.01	<0.01	<0.01	<0.01	<0.01	<0.01	<0.01	<0.01	<0.01	<0.01	<0.01	<0.01	
Carbon dioxide (mg/g)	0.18	0.61	1.19	0.70	0.61	0.49	0.34	0.50	0.63	0.90	0.63	0.56	0.79	1.26	1.21	1.32	1.53	
Methane (mg/g)	0.0	2.8	4.2	9.9	14.0	6.4	9.4	18.2	26.8	33.8	11.9	19.8	29.4	48.5	129.2	122.9	179.4	212.9
C_2–C_5 (mg/g)	0.0	13.5	23.3	51.8	68.1	35.0	48.6	83.5	129.8	156.5	72.0	122.6	160.8	272.2	343.2	343.5	290.5	251.4
C_6–C_{14} (mg/g)	247.5	210.6	302.0	395.6	427.9	330.3	349.6	401.8	495.1	495.4	483.7	444.3	420.4	414.6	22.3	24.4	13.9	8.3
C_{15+} (mg/g)[a]	721.1	764.8	696.1	456.2	453.0	629.3	519.7	410.2	251.9	211.9	437.6	333.1	250.4	148.6	191.6	150.5	200.8	220.6
Pyrobitumen (mg/g)	0.0	20.0	26.4	23.9	51.5	32.8	35.6	32.4	81.9	102.4	48.8	65.3	80.8	138.9	295.5	270.2	353.4	398.8
Total (mg/g)[b]	968.6	1011.9	1052.6	938.6	1015.1	1034.3	963.4	946.5	986.1	1000.6	1055.0	985.7	942.3	1023.7	983.3	912.7	1039.5	1093.7
Resins (mg/g)	122.0	147.6	132.8	116.3	128.3	146.7	129.2	100.7	86.3	73.1	100.3	98.3	78.3	80.7	0.0	0.0	0.0	0.0
Asphaltenes (mg/g)	15.3	14.1	14.0	16.6	13.5	18.3	10.5	7.2	10.8	3.5	13.8	7.0	6.3	10.5	0.0	0.0	0.0	0.0
Aromatics (mg/g)	265.8	252.5	272.2	236.4	252.8	250.3	252.8	264.0	267.5	278.2	302.7	271.9	301.5	316.5	198.8	155.4	209.7	225.7
Saturates (mg/g)	565.6	561.1	579.2	482.4	486.2	544.2	476.9	440.1	382.2	352.1	504.4	399.9	284.5	155.2	14.1	18.4	3.7	1.6
Aromatic/Aliphatic	0.5	0.5	0.5	0.5	0.5	0.5	0.5	0.6	0.7	0.8	0.6	0.7	1.1	2.0	14.1	8.4	57.2	144.2
Pristane/*n*-C17	1.46	1.17	1.03	0.67	0.48	0.85	0.69	0.41	0.13	0.07	0.46	0.29	0.08	0.1	0	0	0	0
Phytane/*n*-C18	1.13	0.92	0.8	0.53	0.4	0.67	0.55	0.33	0.12	0.07	0.37	0.23	0.07	0.09	0	0	0	0
Pristane/Phytane	1.44	1.37	1.39	1.4	1.38	1.4	1.39	1.41	1.22	1.22	1.39	1.42	1.22	1.22	0	0	0	0
n-C10/*n*-C30	1.72	3.27	4.13	6.6	7.43	5.2	5.37	8.16	13.79	15.37	7.84	9.39	23.29	50.78	0	0	0	0
n-C16/*n*-C30	4.84	4.84	5.07	6.22	6.31	5.51	6.14	7.67	13.62	16.26	7.45	9.21	28.38	75.26	0	0	0	0
CPI	1.11	1.11	1.12	1.11	1.07	1.11	1.09	1.02	0.93	0.91	1.08	1.07	1.04	0	0	0	0	0
Gas wetness		0.60	0.64	0.63	0.61	0.63	0.62	0.60	0.61	0.60	0.66	0.66	0.64	0.66	0.52	0.53	0.41	0.35
GOR (Scf/Bbl)		59	95	251	328	147	231	448	742	964	305	611	981	2023	10096	12019	11516	11549
% R_o (Easy R_o)	0	1.02	1.08	1.3	1.41	1.13	1.29	1.44	1.59	1.67	1.25	1.37	1.5	1.65	2.34	2.26	2.53	2.83

[a] Includes resins and asphaltenes.

[b] Total = methane + C_{2-5} + C_{6-14} + C_{15+} + pyrobitumen + CO + CO_2 + H_2.

mg/g to $\%R_o \sim 2.3$. By $\%R_o \sim 2.3$, the NSO's yield is zero and the saturate yield of the C_{10+} is less than 15 mg/g. Hence, by $\%R_o \sim 2.3$, the residual C_{15+} fraction is essentially aromatic (Fig. 4). C_{15+} yield increases again to ~220 mg/g by $\%R_o \sim 2.8$ (450 °C, 6 days) which reflects an increase in aromatic yield. The pristane/*n*-C_{17} and phytane/*n*-C_{18} ratios, used as maturity indicators in crude oils, decrease as thermal stress increases (Fig. 5).

The NSO compounds of the C_{15+} fraction were analyzed in an attempt to better understand changes in C_{15+} yield with increasing thermal stress. NSO compound yield increase approximately 20% at 350 °C, 3 days and 4.3 days ($\%R_o = 1.02$–1.08) and 360 °C, 3 days and 6 days ($\%R_o = 1.13$–1.29, Table 1) over the original oil. Most of the increase is noted in the resin fraction of the NSO's. At $\%R_o$ greater than approximately 1.3, NSO compound yield decreases. A portion of the NSO compounds remains stable to $R_o \sim 1.65\%$ before decreasing to a value of zero. Asphaltene pyrolysis experiments confirm that saturate and aromatic hydrocarbons, pyrobitumen and perhaps minor amounts of gas, are generated from asphaltene cracking (Fig. 6).

3.2. Saturate and aromatic hydrocarbon yield ($\sim C_{15+}$)

The saturate hydrocarbon yields remain essentially constant at low levels of thermal stress (350 °C, 3 and 4.3 days, 360 °C, 3 days; Table 1) and decrease at higher levels of thermal stress. Saturates are essentially absent (<15 mg/g) by ~2.3% (Fig. 4). The aromatic hydrocarbon yields remain essentially constant at low levels of thermal stress (350 and 360 °C), generally increase at higher levels of thermal stress (370–400 °C) and then decrease to the lowest values observed at the highest levels of thermal stress. The aromatic/aliphatic ratio remains constant at 0.5 to $\%R_o \sim 1.3$ and then increases to 144 as thermal stress increases to $\%R_o \sim 2.8$ (Fig. 4).

3.3. $C_{6\text{-}14}$ hydrocarbons

As thermal stress increases, the $C_{6–14}$ hydrocarbon yield increases from an initial value of ~247 mg/g to a maximum of ~500 mg/g at% $R_o \sim 1.7$ (Fig. 3). As thermal stress increases above% $R_o \sim 1.7$, the $C_{6–14}$ yield decreases, reaching a value of ~20 mg/g at % $R_o \sim 2.3$ (440 °C, 3 days) and less than 10 mg/g by $\%R_o \sim 2.8$ (450 °C, 6 days). The remaining $C_{6–14}$ fraction is composed of greater than 90% aromatic compounds by $\%R_o \sim 2.3$ and is 100% aromatic by $\%R_o \sim 2.8$.

3.4. Hydrocarbon gases

The $C_{2–5}$ gas yield, methane yield, and thus, the experimental gas/oil ratio (GOR) also increase as thermal stress increases (Fig. 3). $C_{2–5}$ yield reaches a maximum of ~340 mg/g at $\%R_o \sim 2.3$ based on the data

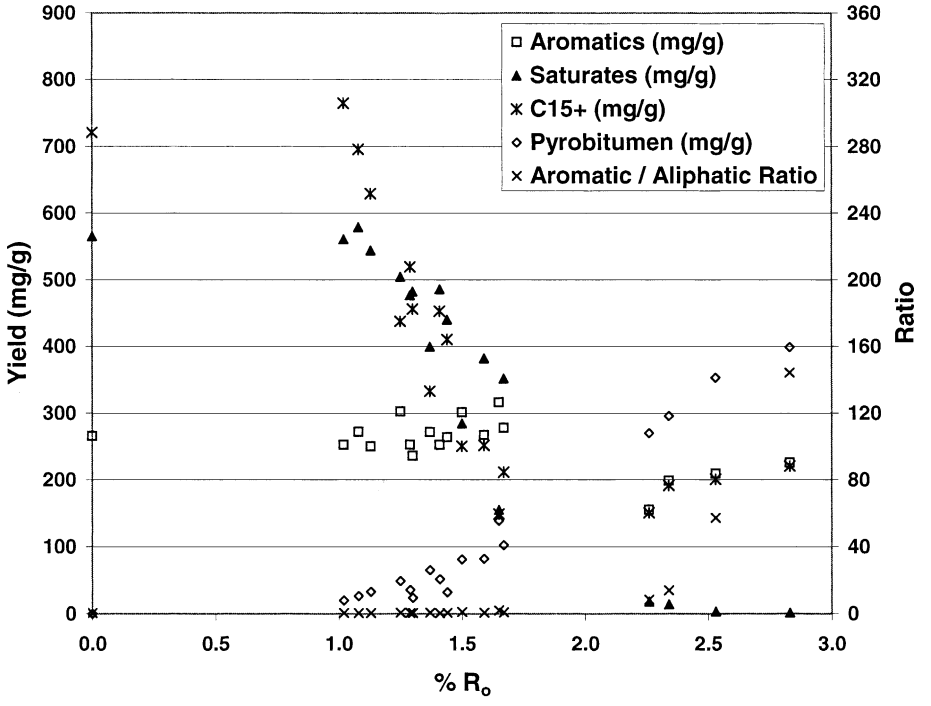

Fig. 4. Changes in C_{15+}, total saturates and total aromatics as a function of increased thermal stress. The stable C_{15+} hydrocarbons at higher maturity are aromatic. Pyrobitumen yield and the aromatic/aliphatic ratio increases at higher levels of thermal stress.

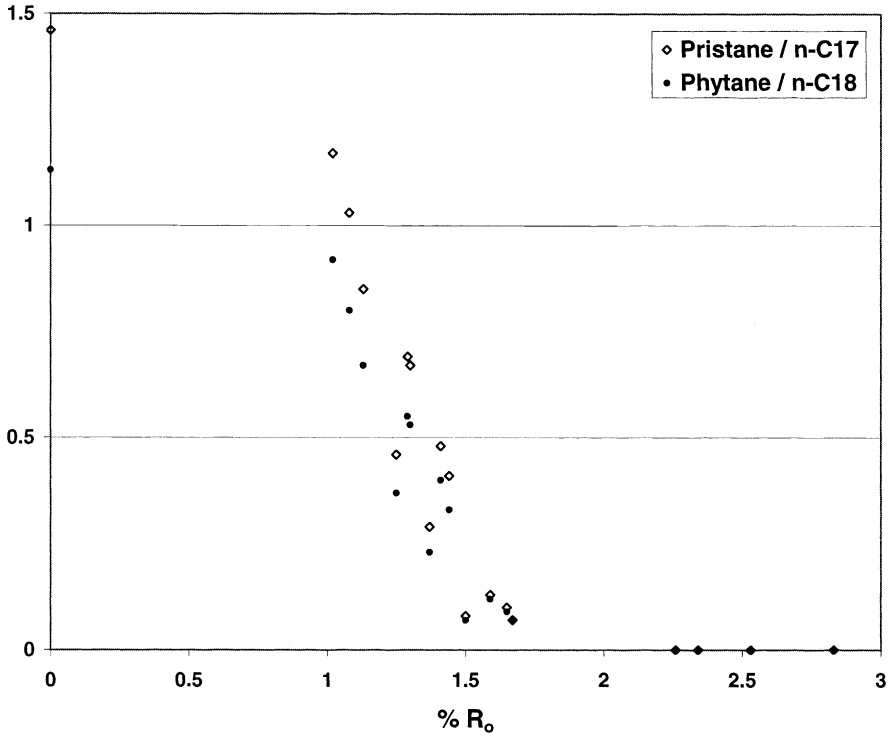

Fig. 5. Trends in experimental pristane/nC$_{17}$ and phytane/nC$_{18}$ ratios with increasing thermal stress. Pristane/nC$_{17}$ and phytane/nC$_{18}$ ratios decrease with increasing thermal stress, similar to what is observed in natural oils and condensates.

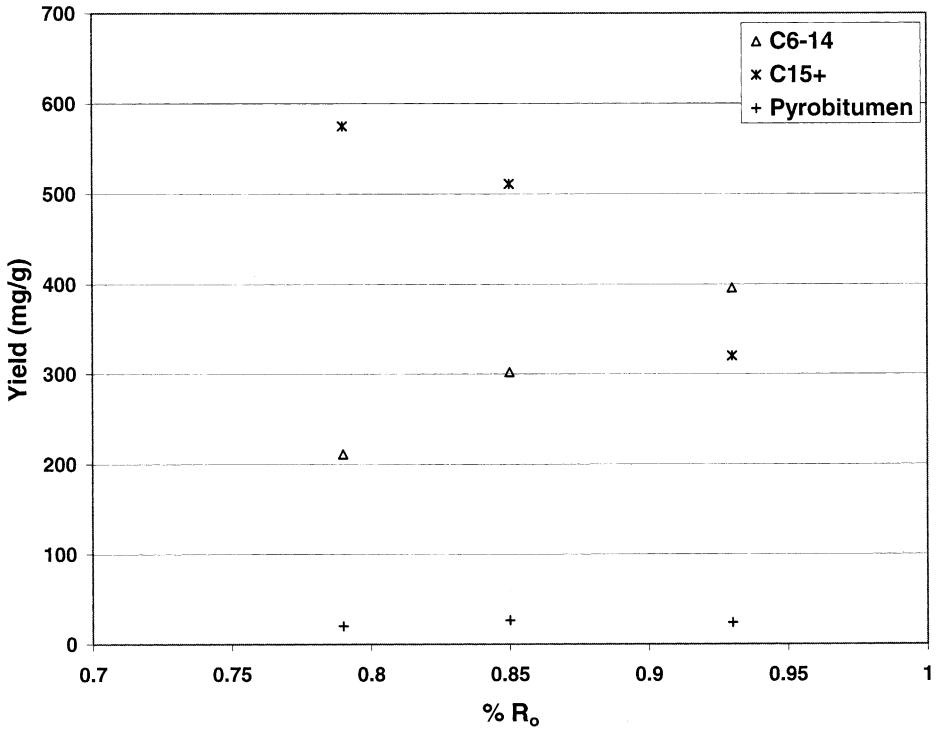

Fig. 6. Asphaltene cracking products demonstrating the generation of hydrocarbons from asphaltenes.

available although it is possible the maximum actually occurs at an equivalent $\%R_o$ value closer to 2.0 (Fig. 7). Above $\%R_o \sim 2.3$, the C_{2-5} yield starts to decrease although cracking of C_{2-5} is not complete by $\%R_o \sim 2.8$. Methane yield increases continually to ~210 mg/g at $\%R_o \sim 2.8$ (450 °C, 6 days) as thermal stress increases although the maximum was not attained. Gas wetness is high throughout the oil cracking experiments, remaining constant at approximately 60%, and decreases by the time thermal stress reaches $\%R_o \sim 2.3$ (440 °C, 3 days; Fig. 8).

3.5. C_{1-5} Hydrocarbon gas carbon isotopes

Methane, ethane and propane carbon isotope values were determined as a function of increasing thermal stress with two trends in $\delta^{13}C$ values observed (Table 2). Early in the pyrolysis process, methane, ethane and propane become enriched in ^{12}C relative to the reference Devonian crude oil. After reaching a $\delta^{13}C$ minimum, methane and propane become enriched in ^{13}C as thermal stress increases (Fig. 9). The level of thermal stress where the most negative $\delta^{13}C$ value is observed is different for each gas. Methane shifts to a trend of ^{13}C enrichment at $\%R_o \sim 1.13$ and propane shifts to ^{13}C enrichment at approximately $\%R_o \sim 1.25$. The change in methane $\delta^{13}C$ is small as thermal stress level increases while changes in propane $\delta^{13}C$ are more pronounced. Ethane behaves differently, ^{12}C enrichment occurs throughout the $\%R_o$ range investigated. The magnitude of difference between $\delta^{13}C_{ethane}$ and $\delta\ ^{13}C_{propane}$ increases in a closed system as thermal stress increases (Fig. 10) like that described for high maturity hydrocarbon gases by James (1983).

3.6. Non-hydrocarbon gases

Non-hydrocarbon gas yields are low and increases as level of thermal stress increases during oil cracking experiments. The contribution to mass balance is limited.

3.7. Pyrobitumen

Pyrobitumen begins to form at low levels of thermal stress during the oil cracking process and continues to form at higher levels of thermal stress as hydrogen-rich hydrocarbon gases are generated (Table 1, Fig. 3). Where the aromatic/aliphatic ratio exceeds ~2 ($\%R_o \sim 1.65$), a corresponding jump in pyrobitumen yield is observed (Fig. 11). A change in slope in pyrobitumen yield is observed at $\%R_o \sim 2.3$.

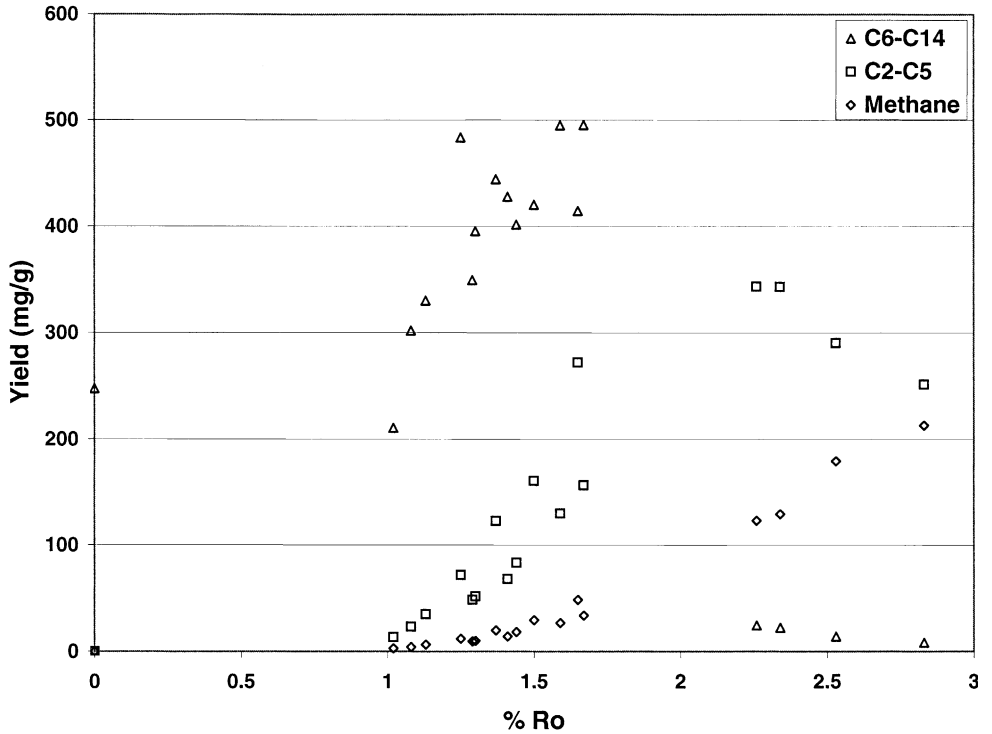

Fig. 7. Changes in C_{6-14}, C_{2-5}, C_1 yield with increase in thermal stress. The point where C_{2-5} yield starts to decrease corresponds with depletion of the C_{6-14} fraction.

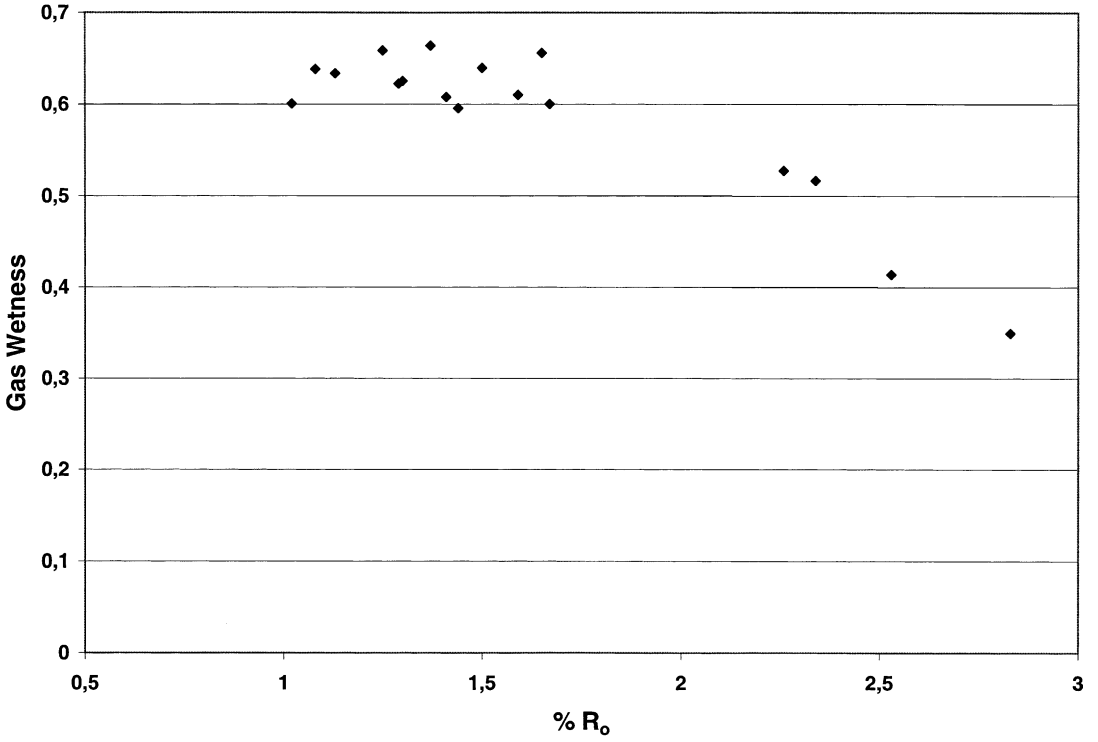

Fig. 8. Experimental gas wetness as a function of increasing thermal stress demonstrating the shift towards low molecular weight products. Experimental gas wetness remains constant at ~64% until C_{2-5} fraction cracking becomes predominant.

4. Discussion

4.1. Controls on oil cracking products and product yield

It is clear from this and other studies that oil cracking is a dynamic process. The redistribution of hydrogen, the availability of reactants and the relative reaction rates between fractions are critical for understanding oil cracking product yields. Relative reaction rates can be determined from this study, but reaction kinetics is not the focus of this paper. The reaction scheme of Fig. 2 is presented to aid the reader in visualizing the reactions discussed. The results of this oil pyrolysis study are consistent with what others have reported; HMW C_{15+} compounds (including NSO's) crack to form LMW C_{6-14}, C_{2-5}, C_1, and pyrobitumen fractions with increasing thermal stress (Bjoroy et al., 1988; Ungerer et al., 1988; Behar et al., 1991, 1992; Horsfield et al., 1992; Kuo and Michael, 1994; Pepper and Dodd, 1995; Schenk et al., 1997; Tsuzuki et al., 1999). Evidence for generation of LMW hydrocarbons from C_{15+} cracking comes from a corresponding increase in C_{6-14}, C_{2-5}, C_1, and pyrobitumen yield (mg product/g original oil) as C_{15+} yield decreases (Fig. 3). This is consistent with previous work that demonstrated that short chain *n*-alkanes have greater thermal stability than long chain *n*-alkanes (Fabuss et al., 1964). Furthermore, decreases in the pristane/nC_{17} and phytane/nC_{18} ratios (Fig. 5) demonstrate that branched alkanes are less stable than *n*-alkanes (Fabuss et al., 1964) and contribute significantly to LMW hydrocarbon formation during the initial stages of oil cracking.

Table 2
Gas carbon isotope values for gases generated during oil pyrolysis at various temperatures and lengths of time[a]

Sample	*T* (°C)	Time (days)	Methane $\delta^{13}C$ (‰)	Ethane $\delta^{13}C$ (‰)	Propane $\delta^{13}C$ (‰)	$\Delta\delta^{13}C_{ethane}-\delta^{13}C_{propane}$
315	350	3	−42.64	ND	−34.56	ND
316	350	4.3	−44.42	−38.32	−36.84	−1.48
308	360	3	−44.23	−38.79	−36.91	−1.88
320	370	3	−44.2	−38.95	−37.13	−1.82
306	360	6	−44.03	−38.78	−37.0	−1.78
312	350	12	−43.87	−38.28	−36.9	−1.38
321	380	3	−43.93	−39.25	−36.87	−2.38
310	350	20.3	−43.6	−38.52	−36.96	−1.56
301	360	12	−43.78	−38.87	−37.01	−1.86
323	390	3	−45.37	−39.49	−36.16	−3.33
303	360	24	−43.52	−39.25	−36.86	−2.39
325	400	3	−43.67	−38.9	−35.41	−3.49
305	360	33.3	−43.45	−39.53	−36.63	−2.9

[a] $\delta^{13}C$ relative to Pee Dee Formation belemnite.

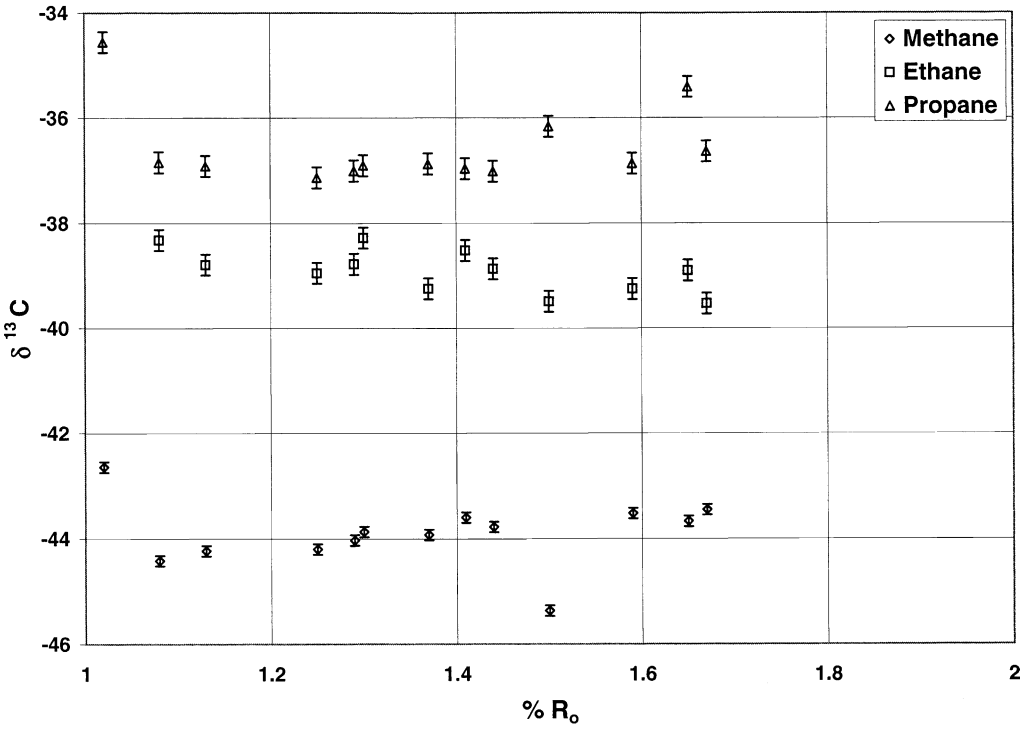

Fig. 9. Changes in methane, ethane and propane $\delta^{13}C$ as a function of increasing thermal stress. At higher levels of thermal stress, ethane and propane begin to diverge.

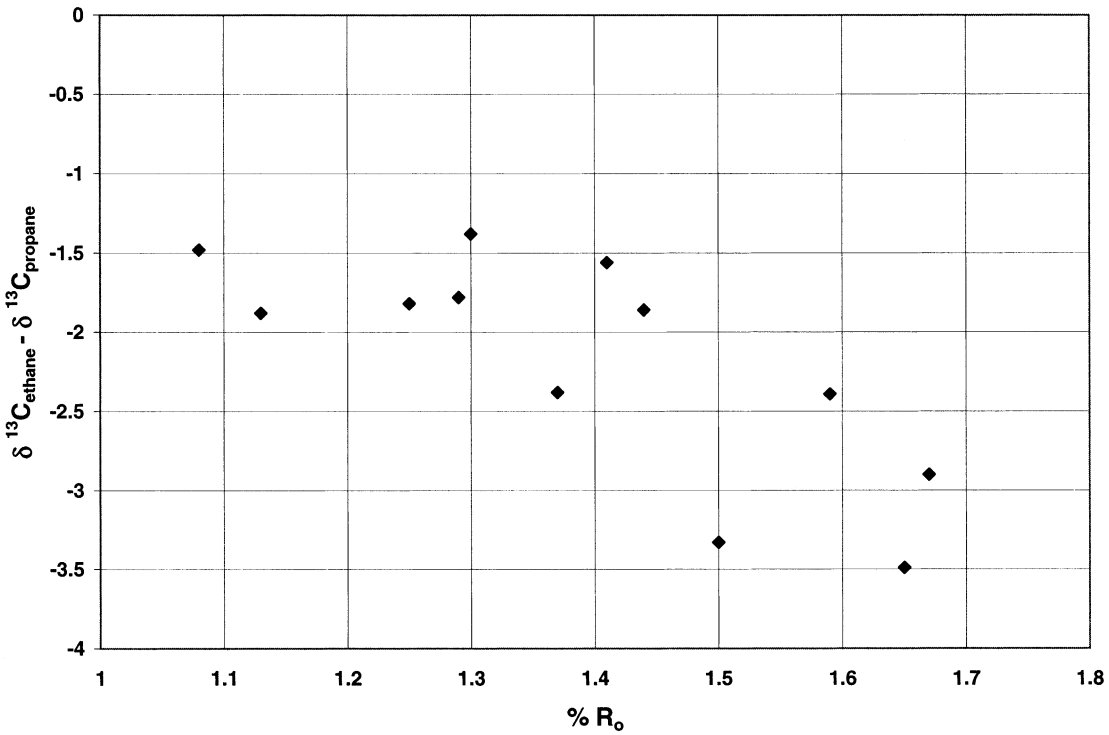

Fig. 10. The $\delta^{13}C_{ethane}$–$\delta^{13}C_{propane}$ difference increases with increasing thermal stress in closed systems. This suggests natural gas maturity interpretations based on isotope differences must also consider system openness.

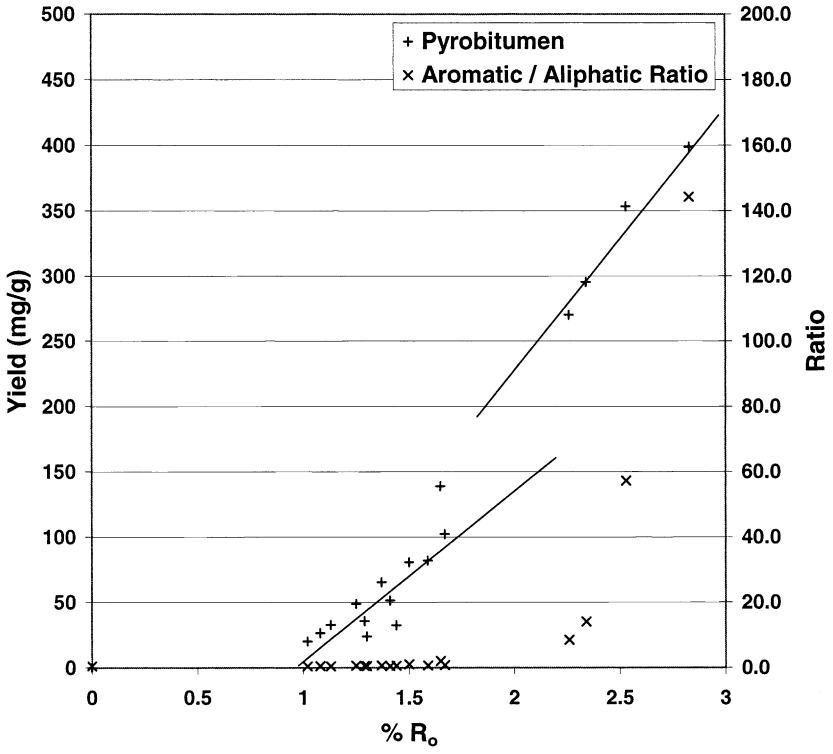

Fig. 11. Pyrobitumen yield and change in aromatic/aliphatic ratio. The slope of the pyrobitumen yield curve changes as the aromatic/aliphatic ratio increases, suggesting an aromatic hydrocarbon control on pyrobitumen yield.

Elemental balance strongly controls the products formed during oil cracking. Methane (H/C = 4) and graphite (100% C) are the thermodynamically stable products expected from oil cracking (Takach et al., 1987). When products with a H/C ratio higher than the reactant are formed, elemental balance requires products with a H/C ratio lower than the reactant also be formed in equal proportion, provided the system is closed and no other source of hydrogen is present. Hence, during C_{15+} (H/C ~ 1.6) cracking, increases in the amount of C_{6-14} (H/C ~ 1.8), C_{2-5} (H/C ~ 2.4) and C_1 (H/C = 4) generated and the experimental gas/oil ratio (Figs. 3 and 12) are offset with increases in the amount of pyrobitumen formed (H/C < 1) and the aromatic/aliphatic ratio of the residual oil (Fig. 4). Within the framework used in this study to describe the oil cracking process, C_{6-14} and C_{2-5} are intermediate products that react further, resulting in increased methane and pyrobitumen yield. Pyrobitumen, the precursor to graphite, acts as a hydrogen donor and continues to become carbon-enriched as thermal stress increases (Behar et al., 1991, 1992).

The amount of C_{6-14}, C_{2-5}, C_1 and pyrobitumen fractions formed during oil cracking is a more complicated issue. Reactant availability (C_{15+}, etc.) and reaction rates control the maximum yield of each fraction. There is considerable overlap in the cracking of the C_{15+}, C_{6-14} and C_{2-5} fractions during oil cracking. Oil cracking pyrolysis products accumulate either because the rate of formation of a product is greater than the rate of cracking or because it is a stable end product and cannot crack further. Intermediate oil cracking product yields decrease because the amount of product formed from a reactant is less than the amount of product continuing to crack. Yield of a product will continue to increase within thermodynamic limits, until a reactant is depleted (Fig. 3). Methane and pyrobitumen are exceptions and increase continually as thermal stress increases because they are stable end products, under the experimental conditions imposed.

Similar factors control the product yield in confined kerogen pyrolysis experiments such as MSSV (Horsfield et al., 1989), gold tube (Behar et al., 1992) and hydrous pyrolysis (Lewan, 1985) where overlap of primary hydrocarbon generation from kerogen and secondary cracking of oil products and the relative rates of these processes also control hydrocarbon yields.

4.2. C_{15+} hydrocarbon and NSO compound fractions

The relationship between the C_{15+} hydrocarbons and the NSO compounds is intimately intertwined. Saturated hydrocarbon yield decreases as thermal stress increases, reflecting the cracking of C_{15+} saturates to

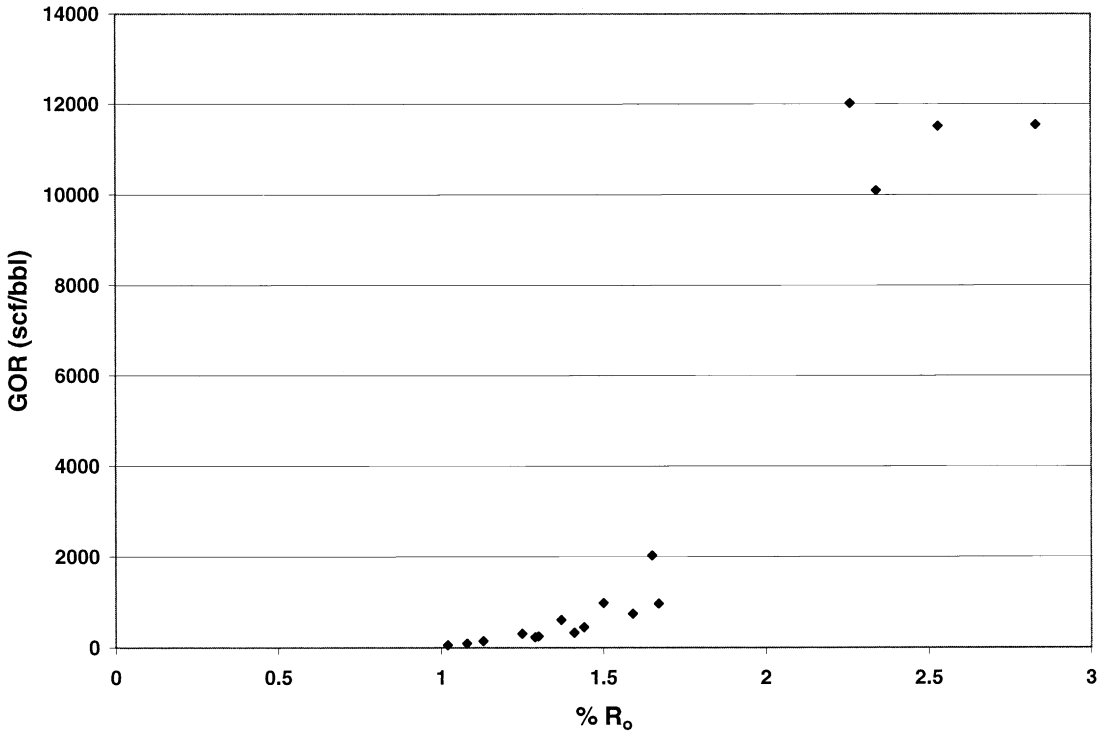

Fig. 12. Changes in experimental gas–oil ratio as thermal stress increases, demonstrating a shift towards lower molecular weight hydrocarbon products.

C_{6-14} saturates, aromatic hydrocarbons and gas. The evolution of aromatic yield throughout oil cracking is a complicated interplay between aromatic hydrocarbon generation from NSO compound cracking, aromatization of the oil during oil cracking and pyrobitumen precipitation. Aromatic yield appears to be controlled primarily by aromatization of the saturate fraction and pyrobitumen precipitation and secondarily from NSO compound cracking due to the small total amount of such compounds in the original oil (Fig. 4). NSO compound cracking and aromatization of the saturated hydrocarbon fraction explains the increase in aromatic yield to $\%R_o \sim 1.65$. The significant drop in aromatic yield between approximately $\%R_o = 1.65$–2.3 corresponds with depletion of the saturated hydrocarbons, that are precursors for aromatic hydrocarbons, and pyrobitumen formation. The correspondence demonstrates that aromatization of saturates is a significant process controlling aromatic compound yield and that once the saturate fraction is depleted, pyrobitumen formation is the dominant control on aromatic yield. To account for the increase in aromatic hydrocarbon yield prior to depletion of saturated hydrocarbons, the rate of aromatization of saturates must be greater than the rate of pyrobitumen precipitation. When the aromatic hydrocarbon precursor is depleted, pyrobitumen formation becomes the primary control on aromatic depletion, resulting in the decrease observed between $\%R_o \sim 1.7$–2.1 (Fig. 4). At $\%R_o > 2$, aromatic yield increases again, corresponding with condensation of the C_{2-5} gas fraction. The accumulation of aromatic compounds again shows the rate of C_{2-5} removal is greater than the rate of pyrobitumen formation. At this point, the products of oil cracking are limited to hydrocarbon gas through cracking of aromatic alkyl side chains and pyrobitumen through aromatic condensation reactions.

A portion of the C_{15+} fraction, dominated by aromatic compounds, is stable to high levels of thermal stress as demonstrated by yields of approximately 200 mg/g to $\%R_o \sim 2.8$ and an increase in the aromatic/aliphatic ratio (Fig. 4). Behar et al. (1999, 2002) demonstrated aromatic compounds are more stable at pyrolysis conditions relative to saturated hydrocarbons, whereas at geologic conditions, saturated hydrocarbons are more stable than aromatic hydrocarbons. The kinetics of aromatic hydrocarbon and saturated hydrocarbon cracking control this change in relative stability. The results of this study are consistent with the findings of Behar et al. (1999, 2002). The detection of saturate-rich hydrocarbons at great depths and high temperatures in nature further supports the greater stability of saturated hydrocarbons at geologic conditions (Price et al., 1979, 1981; Thompson, 1983, 1987; Tissot and

Welte, 1984; Claypool and Mancini, 1989). The preference for pyrobitumen formation via second order aromatic condensation reactions over the first order scission reactions that proceed more rapidly at high temperature pyrolysis conditions also helps to explain the predominance of saturates at high temperatures in natural systems (Horsfield et al., 1992).

An increase in NSO compounds yield over original oil values was observed during the initial stages of oil cracking (Table 1, Fig. 13). The cracking of NSO compounds, comprising approximately 13% of the original oil, is a likely source for saturate hydrocarbons during oil cracking. Asphaltene pyrolysis results from this study (Fig. 6) and NSO compound pyrolysis experiments (Behar and Pelet, 1988; Jones et al., 1988; Bjoroy et al., 1988; Ungerer et al., 1988; Elrod, 1991) confirm saturate and aromatic hydrocarbons, perhaps small amounts of gas hydrocarbons and pyrobitumen are generated as NSO compounds crack (Behar et al., 1992; Horsfield et al., 1992). The NSO compound yield increases slightly at 350 °C, 3 days and 4.3 days ($\%R_o = 1.02$–1.08) and 360 °C, 3 days $\%R_o = 1.13$, Table 1) over the original oil before decreasing at higher levels of thermal stress. Thus, the increase of NSO yield over the original oil is unexpected and appears contradictory given that NSO cracking is generally viewed as a source of saturated and aromatic hydrocarbons during the early stages of oil cracking. Most of the increase is noted in the resin fraction of the NSO compounds. We believe the increase in NSO compound yield is due to formation of a pyrobitumen precursor at low levels of thermal stress during the pyrolysis experiments. This pyrobitumen precursor remains with the NSO compound fraction during resin and asphaltene analysis. Most likely, the pyrobitumen precursor has a condensed aromatic structure, different from the original NSO compounds present in the oil, but not large enough to form an insoluble pyrobitumen residue. Thus, the increase in NSO yield is interpreted to result from formation of "NSO-compound-like" material during oil cracking and precipitates with the NSO compounds during NSO analysis, but is chemically different from the NSO compounds that crack to form saturate and aromatic hydrocarbons.

NSO compounds that persist to at least $\%R_o \sim 1.65$ are also interpreted to be pyrobitumen precursors. Alternatively, Rhamani et al. (2002) showed the kinetics of asphaltenes to coke conversion in maltenes is significantly affected by the composition of the maltenes. Asphaltenes generate less coke in the presence of aromatic hydrocarbons and the rate of asphaltenes conversion to coke is decreased. Hence, the persistence of NSOs in this study may also be attributed to the increased aromatic content of the oil at higher levels of

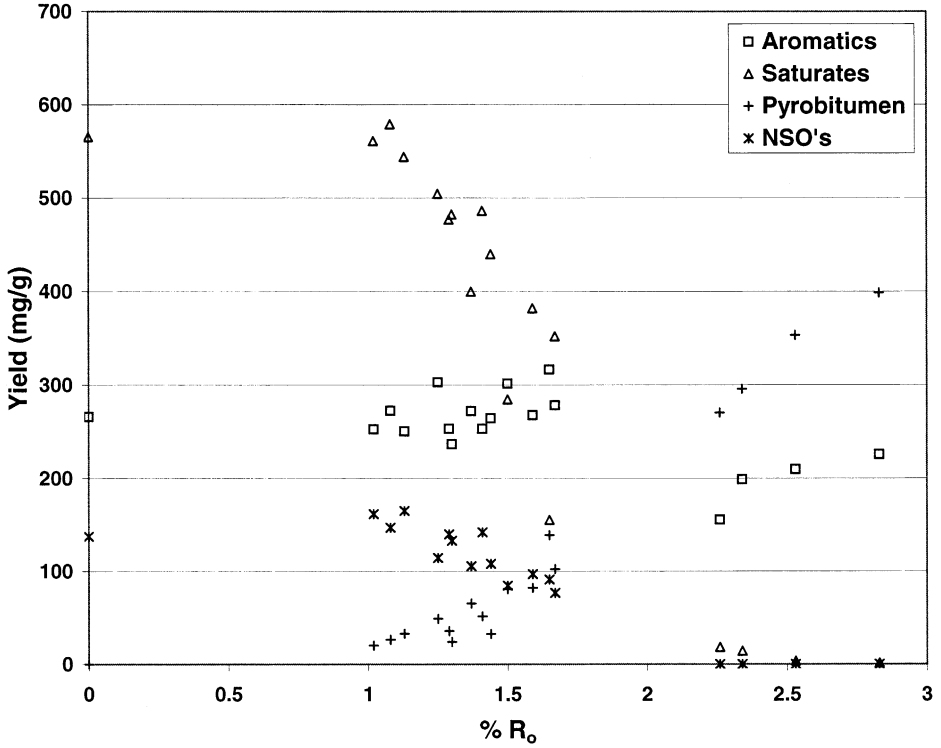

Fig. 13. The relationship between total saturate yield, total aromatic yield and pyrobitumen yield. Aromatization of saturates is a significant process and controls, in part, pyrobitumen yield.

thermal stress. If this is the case, the presence of NSOs at high levels of thermal stress may in part be an artifact of pyrolysis.

In a study of thermochemical sulfate reduction within the Jurassic Smackover Formation, Sassen (1988) noted an increase in resin content with increasing thermal maturity in oils and condensates. We suspect the increase in NSO compound content observed by Sassen (1988) is not only a result of concentration during oil cracking, but also due to formation of sulfur-containing proto-pyrobitumen by aromatization and condensation reactions with the products of thermochemical sulfate reduction.

NSO compound cracking is a significant process in the formation of petroleum from source rocks (Ishiwatari et al., 1976, 1977; Lewan, 1985; Hill et al., 1999). NSO compounds as a source of hydrocarbons during oil cracking has broad implications for natural systems. Clearly, all oils are not NSO-rich, but for those NSO-rich reservoired oils, cracking of these compounds could lead to generation of a higher API gravity oil plus gas. In this case, the reservoirs containing NSO-rich oils could be thought of as a source for lighter, higher API gravity oil, much like shales are considered sources of oils. Furthermore, maturation of NSO-rich oils in reservoirs leading to high API gravity oils may be an important process in some circumstances.

4.3. C_{6-14} fraction

The C_{6-14} fraction has three precursors, the C_{15+} saturates, the C_{15+} aromatics and the NSO compounds. C_{6-14} product accumulates during oil cracking because the rate of C_{6-14} formation is greater than the rate of C_{6-14} cracking. The maximum C_{6-14} yield attained occurs where C_{15+} yield reaches a minimum ($\sim$150 mg/g, $\%R_o \sim 1.7$) and corresponds with nearly complete depletion of C_{15+} saturate compounds (Fig. 14). In other words, the C_{15+} reactant is depleted of C_{6-14} generation potential, limiting the C_{6-14} yield. This observation shows C_{15+} saturates are the primary source for the C_{6-14} fraction and illustrates the strong interdependence of precursor availability and relative cracking rates in determining oil cracking product yield. This does not imply that C_{6-14} cracking is not initiated until C_{15+} is no longer available, but rather that the reactant C_{15+} reservoir is depleted to the extent that more C_{6-14} is cracking than is accumulating. C_{15+} and C_{6-14} cracking occur simultaneously, but C_{15+} cracking occurs at a greater rate. The result is accumulation of C_{6-14} until C_{15+} precursor depletion occurs, at which point C_{6-14} cracking becomes the dominant process. The primary C_{6-14} cracking products are C_1, C_{2-5} and pyrobitumen.

A complete study of the hydrocarbon potential of NSO compounds was not performed so it is difficult to assess the total C_{6-14} contribution from these compounds. However, considering that NSO compounds make up $\sim$13% of the original oil and that NSO cracking results in C_1, C_{2-5}, C_{6-14}, C_{15+} and pyrobitumen products, the contribution of NSO compounds to oil cracking products is secondary to hydrocarbon cracking. Similarly, the original oil is saturate-rich (aromatic/aliphatic ratio $\sim$0.5) making the contribution of C_{15+} aromatic cracking secondary to saturated hydrocarbon cracking.

4.4. C_{2-5} fraction

The C_{2-5} fraction precursors include C_{15+} saturates, C_{15+} aromatics (including alkyl aromatics), the C_{6-14} fraction and perhaps the NSO compounds based on accumulation of C_{2-5} during C_{15+} cracking and C_{6-14} cracking. Indirectly, the C_{15+} precursor is controlling the amount of C_{2-5} by influencing the C_{6-14} yield. Correspondence of the C_{2-5} fraction maximum at $\%R_o \sim 2.3$ with depletion of the C_{6-14} fraction demonstrates that C_{2-5} maximum yield is controlled by the amount of precursor C_{6-14} available and the rate of C_{6-14} cracking (C_{2-5} generation) versus C_{2-5} cracking (Fig. 7). C_{2-5} accumulates because the rate of C_{2-5} generation (C_{15+} and C_{6-14} cracking) is greater than the rate of C_{2-5} cracking. The decline in C_{2-5} yield occurs because the amount of C_{2-5} generated from C_{6-14} cracking is less than the amount of C_{2-5} cracking to methane plus pyrobitumen. Again, we see evidence of multiple reactions occurring simultaneously, in this case C_{6-14} cracking and C_{2-5} cracking with the relative rates of reaction acting as the control on product accumulation.

4.5. Methane

Methane is a product of C_{15+} hydrocarbon, C_{6-14} and C_{2-5} and perhaps NSO cracking and accumulates because it is a stable end product. The rate of methane generation varies depending on the reactant and the level of thermal stress. Hydrogen balance controls the total methane yield in a closed system with no other hydrogen source available. For example, a saturate-rich oil containing mostly normal and branched saturates ($H = 2n + 2$) where n is the number of carbons in the compound) might be expected to have greater methane potential than oil with a greater proportion of cyclic compounds ($H = 2n$).

4.6. Gas wetness

The composition of gas generated from oil cracking remains nearly constant (60–65 vol.% C_{2-5}) until $\%R_o \sim 2.3$ when C_{2-5} yield and gas wetness decrease (Table 1, Fig. 8). This result demonstrates that the gas

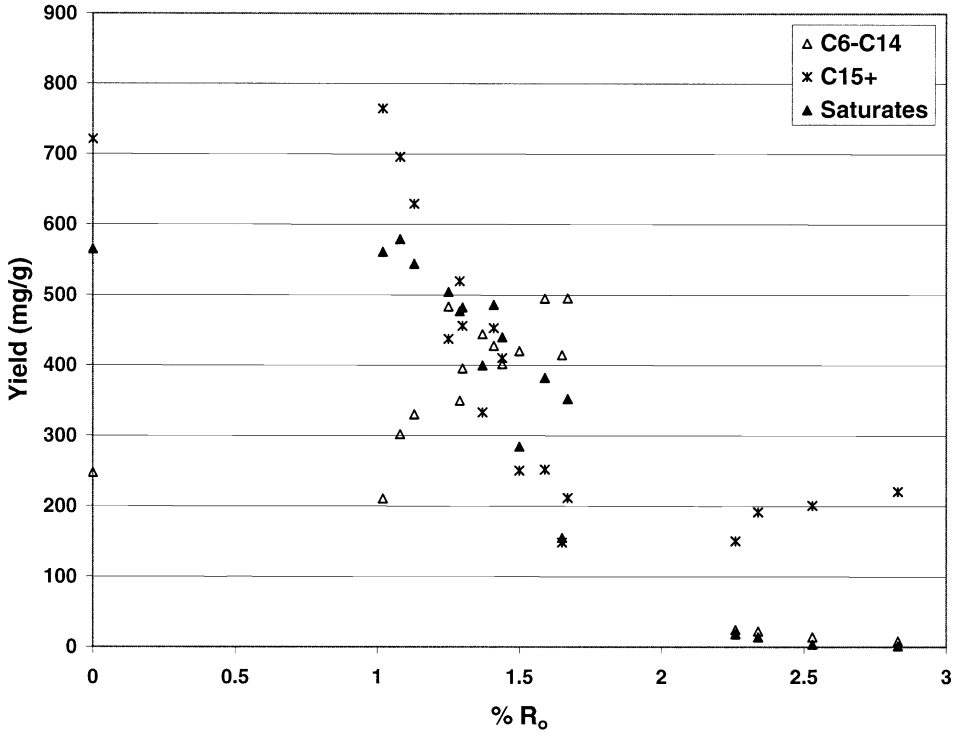

Fig. 14. $C_{6–14}$ maximum corresponds with the complete aromatization (depletion) of C_{15+} fraction and depletion of the total saturated hydrocarbon reactant. This demonstrates the importance of precursor availability and relative reaction rate (C_{15+} cracking $> C_{6–14}$ cracking) on $C_{6–14}$ yield.

derived from C_{15+} and $C_{6–14}$ cracking has essentially the same composition and rates of formation throughout the oil cracking process, at least until the $C_{2–5}$ fraction begins to crack. Oil cracking experiments provide a framework for interpreting oil and natural gas data. The gas formed by pyrolysis has considerably lower methane content (C_1 ~35–40%) than reservoired natural gases (C_1 ~60–95+%) (Mango, 1997, 2001; Snowdon, 2001). If pyrolysis experiments simulating oil cracking do represent the gas generation processes occurring in reservoirs, then understanding these and other natural processes that alter gas compositions is essential. Snowdon (2001) summarized the factors and processes that can influence natural gas composition. These factors and processes include the chemistry of the source kerogen, gas generation reaction mechanisms, thermal stress and thermal maturity, migration fractionation, partitioning of gas components between gas and oil phases, thermochemical sulfate reduction, biodegradation and hydrate formation. Snowdon (2001) notes that gases collected from drill cuttings of fine-grained rocks are enriched in C_{2+} components (80% ± 10) and argues that cuttings gas composition is representative of gas generated during kerogen cracking. These results corroborate the findings of Price and Schoell (1995) who also demonstrated the presence of wet gas in the Bakken Shale of the Williston Basin and are consistent with pyrolysis results. Snowden also found that cuttings gas is C_{2+} enriched to significant burial depths and temperatures demonstrating that wet gas dominates sedimentary sequences. Likewise, Snowdon argues that since gases have been through a series of processes from generation through migration and production that may alter gas composition, the composition of produced gases is not representative of the composition of gases at the time of generation.

Significant efforts have already been made in understanding migration effects (Schoell, 1995; Price and Schoell, 1995). Migration fractionation and $C_{2–4}$ solubility in oil were proposed as the primary processes to account for differences in shale gas and reservoired gas composition in the Williston Basin (Price and Schoell, 1995). The mixing of late stage, methane-rich gas with wet gas generated during main stage hydrocarbon generation is another process that may contribute to the occurrence of methane-rich reservoired gases. The generation of methane-enriched gas from late stage (post-oil generation) kerogen cracking has been documented in laboratory experiments (Chung and Sackett, 1979; Cambell et al., 1980a,b; Price, 1995; Behar et al., 1995; Cramer et al., 2001; Lorant and Behar, 2002). Mixing processes were significant in the evolution of mid-continent gases and help to explain the composition of gases (Jenden et al., 1988).

Gas generated through catalytic cracking either by interaction of organic matter with minerals (Tannenbaum and Kaplan, 1985) or transition metals (Mango and Hightower, 1997; Mango and Elrod, 1998) has been proposed. Clay mineral influences on hydrocarbon generation are significant in the laboratory. We know that organic compounds will adsorb to mineral surfaces in both natural systems and laboratory experiments and that smectitic clay minerals can significantly alter hydrocarbon composition in laboratory experiments with kerogen (Tannenbaum and Kaplan, 1985; Tannenbaum et al., 1986; Huizinga et al., 1987a,b). Up to 5× the amount of C_{1-6} was generated from kerogen in the presence of montmorillonite as compared to kerogen alone (Tannenbaum and Kaplan, 1985). C_{1-6} generation was reduced in the presence of illite when compared to montmorillonite in the studies by Tannenbaum and Kaplan (1985) contrary to experimental results from Espitalie et al. (1980), who showed illite to have significant effect on the generation of gas and condensate products from kerogen. Illite, mixed layer illite–smectite, kaolinite and chlorite are clays commonly found in hydrocarbon reservoirs. Water is present in shales and hydrocarbon reservoirs and has been shown to significantly diminish the effect of clays on hydrocarbon generation in pyrolysis experiments. These observations have been used to dismiss the significance of clay minerals in hydrocarbon generation. Mango (2001) provided an excellent summary of alternatives to account for the difference in composition between pyrolysis gas and natural gas. The role of transition metal catalysts in the experimental conversion of oil to methane has been demonstrated (Mango and Elrod, 1998), but its quantitative importance in natural systems is yet to be established. Mango and Hightower (1997) have estimated the half-life of oil to be 350,000 years at 175 °C over dry H_2 activated NiO/SiO_2 catalyst. However, the methane-rich gas generated during pyrolysis in the presence of transition metals is not consistent with the composition of shale gas and does not support the role of transition metals in gas generation. Furthermore, the half-life for conversion of oil to methane is not supported by the persistence of wet gas components in fined grained sediments at 175 °C for millions of years (Snowdon, 2001). Although the experimental transition metal catalyzed gas generation results are intriguing, evidence for these processes in natural systems is lacking.

4.7. Gas isotopes

Methane, ethane and propane carbon isotope values were determined as a function of increasing thermal stress with two trends in $\delta^{13}C$ values observed (Table 2). During early generation in the pyrolysis process, methane, ethane and propane become enriched in ^{12}C relative to the reference Devonian crude oil. Since the oil is topped and no dissolved gas remains, this ^{12}C enrichment appears to be a product of hydrocarbon cracking. After reaching a $\delta^{13}C$ minimum, methane and propane become enriched in ^{13}C as thermal stress increases (Fig. 9). Tang et al. (2000) reported initial enrichment in ^{12}C with increase in thermal stress similar for methane generated during pyrolysis and suggested two or more precursors were contributing to methane generation. The level of thermal stress where the most negative $\delta^{13}C$ value is observed is different for each gas, but the data suggest that the precursors to the gas components become progressively depleted in ^{12}C. Methane shifts to a trend of ^{13}C enrichment at $\%R_o \sim 1.13$ and propane shifts to ^{13}C enrichment at approximately $\%R_o \sim 1.25$. This behavior suggests gas is being generated from multiple sources within the oil precusor. The change in methane $\delta^{13}C$ is small as thermal stress level increases, whereas changes in propane $\delta^{13}C$ are more pronounced. Ethane behaves differently, ^{12}C enrichment occurs throughout the $\%R_o$ range investigated, suggesting that ethane is being derived from a different precursor than methane and propane. After the initial ^{12}C enrichment, the general trend is for methane and propane to become progressively enriched in ^{13}C and for ethane to become progressively enrich in ^{12}C as thermal stress increases. The methane, ethane and propane $\delta^{13}C$ at $\%R_o \sim 1.5$ appears to be anomalous with methane showing the greatest deviation from the apparent data trend. Incomplete release of gases from the cold trap could explain the ^{12}C enrichments for methane and ethane. Further investigation of the gas isotope trends is required to better interpret the observations.

Determining the origin and maturity of natural gases is difficult due to the limited geochemical information one can obtain for gases and the changes that occur due to subsurface alteration processes. Compositional and isotopic data are limited, by definition, for gases and do not always provide unique interpretation. The difference in ethane and propane $\delta^{13}C$ ($\delta^{13}C_{ethane}$–$\delta^{13}C_{propane}$) has been used as a maturity indicator (James, 1983, 1990; Chung et al., 1988; Lorant, et al., 1998). In general, with increasing thermal maturity, the difference between $\delta^{13}C_{ethane}$ and $\delta^{13}C_{propane}$ decreases. For a Type II kerogen, Lorant et al. (1998) showed that in open system pyrolysis, the difference between $\delta^{13}C_{ethane}$ and $\delta^{13}C_{propane}$ decreases with increasing thermal stress, but that in closed system pyrolysis, the difference between $\delta^{13}C_{ethane}$ and $\delta^{13}C_{propane}$ increases with increasing thermal stress. For oil cracking, our results also show that with increasing thermal stress, the difference between $\delta^{13}C_{ethane}$ and $\delta^{13}C_{propane}$ increases in a closed system (Fig. 10). We have evaluated our data within the framework of Prinzhofer and Huc (1995), Prinzhofer et al. (2000) and Lorant et al. (1998). Prinzhofer and Huc (1995) and Prinzhofer et al. (2000) used a $\delta^{13}C_{ethane}$–$\delta^{13}C_{propane}$ vs. C2/C3 ratio to differentiate sources of gas

(Fig. 15). Our experimental results fall within their field of secondary cracking of hydrocarbons. Our oil cracking results confirm those of Lorant et al. (1998) who demonstrated for a Type II kerogen, that the difference between $\delta^{13}C_{ethane}$ and $\delta^{13}C_{propane}$ is a function of system openness as well as level of thermal stress.

James (1983) presented an example from the Delaware-Val Verde Basin demonstrating an increase in the $\delta^{13}C_{ethane}$–$\delta^{13}C_{propane}$ difference at high levels of thermal maturity and attribute this deviation from his calculated maturity trend to oil and wet gas cracking. Our results are certainly consistent with this observation. This brings into question gas maturity interpretations based simply on the difference between $\delta^{13}C_{ethane}$ and $\delta^{13}C_{propane}$ using the methods of James (1983, 1990). As the $\delta^{13}C_{ethane}$–$\delta^{13}C_{propane}$ difference increases with increasing thermal stress in our experiments and in the Delaware-Val Verde example, the interpreted maturity as determined by the James method would continually decrease. James (1983) acknowledged that the high maturity gases of the Delaware-Val Verde are problematic. However, if plotted on the James diagram, the $\delta^{13}C_{methane}$ should plot below the calculated methane line for these high maturity examples, providing a method to distinguish high maturity gases. Problems arise if a high maturity gas derived from hydrocarbon cracking is mixed with biogenic methane. The $\delta^{13}C_{methane}$ signature would be altered such that the gas would have low maturity characteristics leading to an erroneous interpretation. This reinforces the importance of integrating geologic information when interpreting geochemical data and also highlights the need for continued research into the origin of natural gases.

Prinzhofer and Huc (1995) demonstrated ratios of C_{2-5} gas components can be used to estimate gas thermal maturity. Gases generated in this oil cracking study follow the maturity trend defined in their C_2/i-C_4 vs. C_2/C_3 plot (Fig. 15). This provides an alternative or complimentary method to isotope plots for estimating gas thermal maturity and a valuable tool when applied in combination with isotope data.

4.8. Pyrobitumen

Pyrobitumen precursors include the NSO compounds, C_{15+} hydrocarbons, C_{6-14} and C_{2-5} based on pyrobitumen formation during cracking of these components. The increase in pyrobitumen yield with increasing thermal stress coincides with an increase in methane yield and a decrease in C_{15+}, C_{6-14} and C_{2-5} as each of the fractions crack. Pyrobitumen forms by aromatic condensation reactions (Ungerer et al., 1988; Behar et al., 1992) and appears to require an aromatic hydrocarbon intermediate, except when forming from NSO compounds, where a direct path may exist (Fig. 11). Aromatic hydrocarbons are clearly a significant precursor in pyrobitumen formation. This is illustrated by the corresponding decrease in aromatic hydrocarbon yield and depletion of the saturate hydrocarbons (Fig. 13). In order for the aromatic yield to decrease, the reactant contributing to aromatic hydrocarbon formation must be depleted and the aromatics must be converting to other products. In these experiments, the saturate hydrocarbons are first depleted, thus limiting the formation of aromatic hydrocarbons while pyrobitumen formation continues, resulting in depletion in aromatic yield. The result shows aromatic hydrocarbon formation and pyrobitumen formation are occurring simultaneously. A change in slope in the pyrobitumen yield curve occurs where C_{2-5} gas decreases and only aromatic compounds remain in the C_{6+} fraction. Aromatic hydrocarbon formation initially occurs at a greater rate than pyrobitumen formation until the saturated hydrocarbons are depleted. The aromatic content of the original oil and the saturate composition (amount of hydrogen available during oil cracking) controls the pyrobitumen yield. All of the past experimental studies show or suggest pyrobitumen is an important product of oil cracking.

Experimental results show pyrobitumen forms early during oil cracking. In natural systems, aromatic condensation and precipitation of pyrobitumen is called on to explain the decrease in aromatic/aliphatic ratio with increasing maturity. Unless an external source of hydrogen is available (water, mineral or trace element interaction), formation of pyrobitumen is a required consequence of oil cracking in reservoirs. Investigating the distribution of reservoir pyrobitumen will provide constrain on the depth, temperature and pressure conditions for oil cracking and thus, the stability of oil in nature. The key to understanding pyrobitumen distribution in nature is the kinetics of pyrobitumen formation.

4.9. The influence of pressure

Oil cracking experiments were performed at 650 bars pressure in order to simulate reservoir pressures in the Western Canada Sedimentary Basin where oil cracking occurs. The influence of pressure on oil cracking was investigated previously (Hill et al., 1996), who found that cracking rates are enhanced slightly at pressures up to ~600–700 bars as compared to 90 bars, as measured by relative changes in the C_1, C_{2-5}, individual alkane and pyrobitumen fraction yields (Hill et al., 1996). Above pressures of 600–700 bars, yields of all oil cracking products decreased, supporting a retardation or suppression of oil cracking. Changes in oil cracking reaction rates are explained by activation volume effects. We believe reaction mechanisms do not change as pressure increases, because gas wetness does not change significantly and pyrobitumen yield trends follow methane yield. If reaction mechanisms were changing with pres-

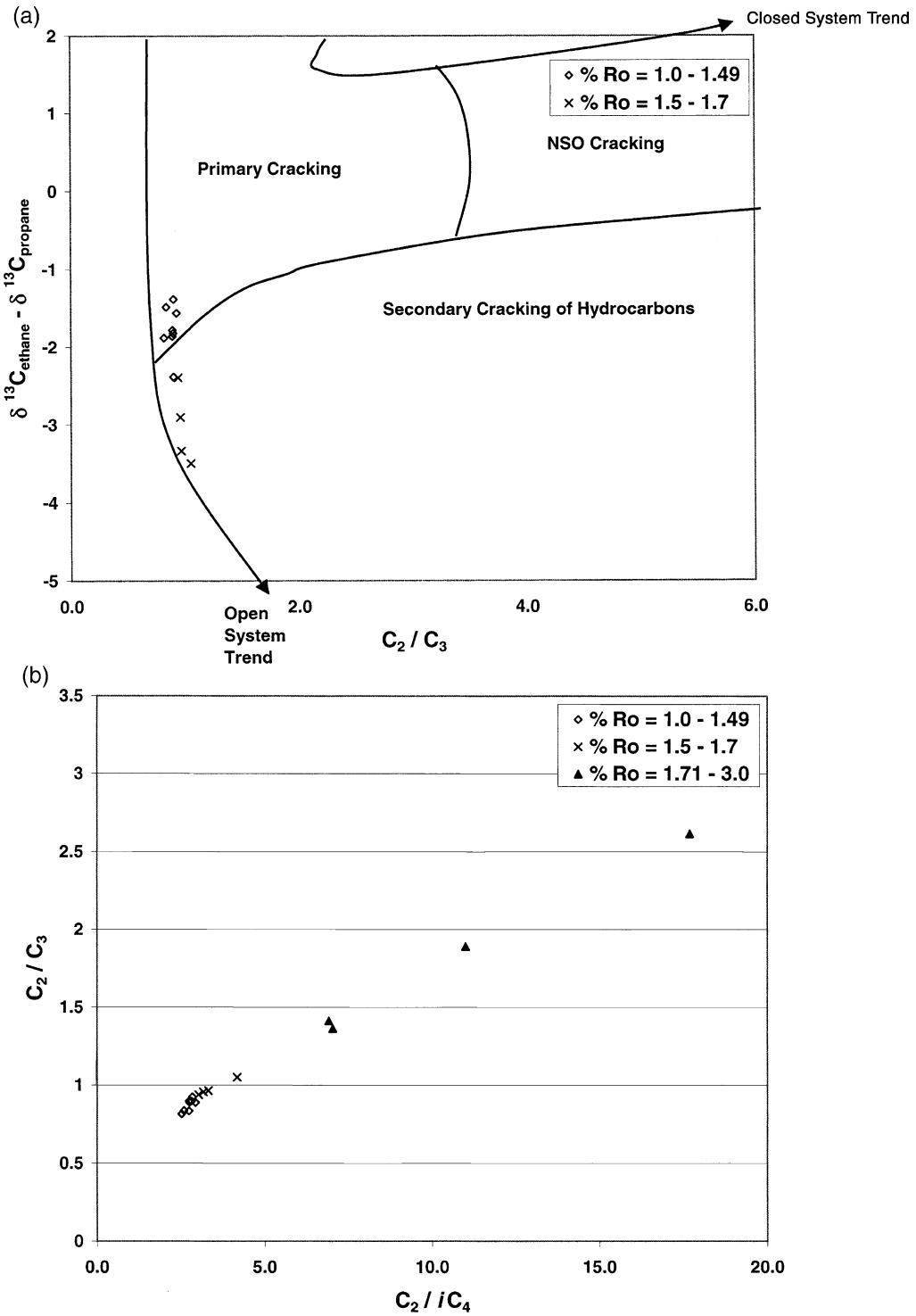

Fig. 15. (a) The $\delta^{13}C_{ethane}$–$\delta^{13}C_{propane}$ vs C_2/C_3 data for these oil cracking experiments plot in the primary and secondary cracking fields of Lorant et al. (1998). The gases that plot in the primary cracking field are from experiments performed at lower thermal stress levels whereas gases plotting in the seconday cracking field are from experiments performed at higher thermal stress levels. Further investigation is needed to confirm the closed system trend they report. (b) A plot of C_2/C_3 vs C_2/iC_4 is maturity sensitive, as reported by Prinzhofer et al. (2000).

sure, one might expect gas wetness to vary or methane and pyrobitumen yield trends to differ due to elemental balance considerations. Thus, simulating oil cracking in the Western Canada Basin with experiments performed at 650 bars means that oil cracking rates are enhanced slightly relative to experiments performed without confining pressure leading to minor increases in product yields. However, the distribution of oil cracking products remains the same as in experiments at lower pressure.

5. Summary

Oil cracking is a complicated, dynamic process involving many different cracking reactions that occur simultaneously. The C_{15+} fraction cracks to $C_{6–14}$, $C_{2–5}$, and C_1 hydrocarbon fractions plus pyrobitumen, the $C_{6–14}$ fraction cracks to $C_{2–5}$ and C_1 gases plus pyrobitumen and the $C_{2–5}$ fraction cracks to C_1 plus pyrobitumen. The relative rates of cracking reactions and amount of reactant available control the yield of final products. Individual oil cracking products accumulate, as long as the reactant oil is available, because either the rate of generation of a product is greater than the rate of cracking of that product or because the product is a stable end member. The $C_{6–14}$ fraction accumulates because the rate of C_{15+} cracking is greater than the rate of $C_{6–14}$ cracking and C_{15+} reactant is not depleted. Likewise, the $C_{2–5}$ fraction increases because the rate of $C_{6–14}$ cracking is greater than the rate of $C_{2–5}$ cracking and the $C_{6–14}$ reactant is not depleted. Methane and pyrobitumen accumulate because they are stable end products. Oil cracking product yields decrease when the amount of product being generated from a reactant is less than the amount of product cracked. Thus, there is a correspondence in decrease of $C_{6–14}$ yield with depletion of C_{15+} saturates and decrease in $C_{2–5}$ yield with depletion of the $C_{6–14}$ fraction. Although NSO compounds crack to yield gas and liquid hydrocarbons, NSO compounds initially increased in our experiments due to formation of pyrobitumen precursor that although chemically different, cannot be separated from the resins and asphaltenes during NSO analysis.

Similar to oils and condensates in reservoirs, pyrolysate isoprenoid/*n*-alkane (pristine/nC_{17} and phytane/nC_{18}) ratios continue to decrease during oil cracking. Unlike oils and condensates in reservoirs, the aromatic/aliphatic ratio continually increased as experimental oil cracking proceeds. Pyrobitumen formed at low levels of thermal alteration in the experiments we conducted and increased in yield as higher levels of thermal stress were achieved. Pyrobitumen in hydrocarbon reservoirs provides a potential indicator for the onset of oil cracking. Understanding the spatial and vertical distribution of pyrobitumen will provide insight into the pressure and temperature conditions necessary for oil cracking in reservoirs, the oil floor and deeper gas potential.

The $C_{1–5}$ hydrocarbon gas fraction from pyrolysis in this study maintains ~65% wetness until the $C_{2–5}$ fraction begins to crack at high levels of thermal stress, whereas natural gases contain from 5 to 35% $C_{2–5}$ components. If gases from these oil pyrolysis experiments are representative of gases generated during oil cracking in nature, then secondary alteration processes are the key to understanding the difference in gas wetness of natural gases and pyrolysis gases and thus, natural gas composition. In this study, methane and propane are initially enriched in ^{12}C, but become enriched in ^{13}C as oil cracking continues, suggesting that the gas was generated from multiple sources. Ethane $\delta^{13}C$ was continually enriched in ^{12}C throughout the $\%R_o$ range of pyrolysis investigated, suggesting that ethane may have a precursor other than methane or propane. The difference between $\delta^{13}C_{ethane}$ and $\delta^{13}C_{propane}$ increases in these experiments with increase in maturity.

Finally, one must consider reaction rate and reactant availability effects on product yield when simulating hydrocarbon generation from kerogen by confined pyrolysis. Product yield is controlled by both the primary generation of hydrocarbons from kerogen and secondary cracking of hydrocarbons. These two processes overlap significantly.

Acknowledgements

This work was performed at UCLA as part of R.J.H.'s dissertation. R.J.H would like to thank the Department of Earth and Space Sciences at UCLA for use of the hydrothermal lab and Chevron Petroleum Technology Company for financial support of the project and use of analytical facilities. Feedback and support on the project from Peter Jenden is gratefully acknowledged. R.J.H would like to thank Jesse Ortiz, Jesse Jamie and Mark Haught for technical support. Mike Lewan, Peter McCabe, Rolando di Primio, Kathy Varnes and an anonymous reviewer provided helpful comments and suggestions that significantly improved the manuscript.

Associate Editor — **L. Schwark**

References

Allan, J., Creaney, S., 1991. Oil families of the Western Canada basin. Bulletin of Canadian Petroleum Geology 39, 107–122.

Barker, C., 1990. Calculated volume and pressure changes during thermal cracking of oil to gas in reservoirs. American Association of Petroleum Geologists Bulletin 74, 1254–1261.

Behar, F., Pelet, R., 1988. Hydrogen transfer reactions in the thermal cracking of asphaltenes. Energy and Fuels 2, 259–264.

Behar, F., Ungerer, P., Kressman, S., Rudkiewicz, J.L., 1991. Thermal evolution of crude oils in sedimentary basins:

experimental simulation in a confined system and kinetic modeling. Revue de l'Institut Francais du petrole 46, 151–181.
Behar, F., Kressman, S., Rudkiewicz, J.L., Vandenbrouke, M., 1992. Experimental simulation in a confined system and kinetic modeling of kerogen and oil cracking. In: Eckardt, C. B., Maxwell, J.R., Larter, S.R., Manning, D.A.C. (Eds.), Advances in Organic Geochemistry, Vol. 19, pp. 173–189.
Behar, F., Vandenbrouke, M., Teerman, S.C., Hatcher, P.G., Leblond, C., Lerat, O., 1995. Experimental simulation of gas generation from coals and a marine kerogen. Chemical Geology 126, 247–260.
Behar, F., Budzinski, H., Vandenbrouke, M., Tang, Y., 1999. Methane generation from oil cracking: kinetics of 9-methylphenanthrene cracking and comparison with other pure compounds and oil fractions. Energy and Fuels 13, 471–481.
Behar, F., Lorant, F., Budzinski, H., Desavis, E., 2002. Thermal stability of alkylaromatics in natural systems: kinetics of thermal decomposition of dodecylbenzene. Energy and Fuels 16, 831–841.
Bjoroy, M., Williams, J.A., Dolcater, D.L., Winters, J.C., 1988. Variation in hydrocarbon distribution in artificially matured oils. Organic Geochemistry 13, 901–913.
Cambell, J.H., Koskinas, G.J., Gallegos, G., Gregg, M., 1980a. Gas evolution during oil shale pyrolysis. 1. Nonisothermal rate measurements. Fuel 54, 718–726.
Cambell, J.H., Gallegos, G., Gregg, M., 1980. Gas evolution during oil shale pyrolysis. 2. Kinetic and stoichiometric analysis. Fuel 54, 727–732.
Chung, H.M., Sackett, W.M., 1979. Use of stable carbon isotope compositions of pyrolytically derived methane as maturity indices for carbonaceous materials. Geochimica Cosmochimica Acta 43, 1979–1988.
Chung, H.M., Gormly, J.R., Squires, R.M., 1988. Origin of gaseous hydrocarbons in subsurface environments: theoretical considerations of carbon isotope distribution. In: Schoell, M. (Ed.), Origins of Methane in the Earth Chemical Geology, Vol. 71, pp. 97–103.
Claypool, G.E., Mancini, E.A., 1989. Geochemical relationships of petroleum in Mesozoic reservoirs to carbonate source rocks of Jurassic Smackover Formation, Southwest Alabama. American Association of Petroleum Geologists Bulletin 73, 904–924.
Cramer, B., Faber, E., Gerling, P., Krooss, B.M., 2001. Reaction kinetics of stable carbon isotopes in natural gas—insights from dry, open system pyrolysis experiments. Energy and Fuels 15, 517–532.
Domine, F., 1989. Kinetics of hexane pyrolysis at very high pressures. 1. Experimental study. Energy and Fuels 3, 89–96.
Domine, F., Marquaire, P.M., Mueller, C., Come, G.M., 1990. Kinetics of hexane pyrolysis at very high pressures, 2. Computer modeling. Energy and Fuels 4, 2–10.
Domine, F., 1991. High pressure pyrolysis of n-hexane, 2,4-dimethylpentane and 1-phenylbutane. Is pressure and important geochemical parameter? Organic Geochemistry 17, 619–634.
Domine, F., Enguehard, F., 1992. Kinetics of hexane at very high pressures—3. Application to geochemical modelling. Organic Geochemistry 18, 41–49.
Domine, F., Dessort, D., Brevart, O., 1998. Towards a new method of geochemical kinetic modeling: implications for the stability of crude oils. Organic Geochemistry 28, 597–612.
Elrod, L., 1991. Application of asphaltene pyrolysis to the characterization of degraded crude oils. In: Meyer, R.F. (Ed.), Heavy Crude and Tar Sands—Petroleum for the 21st Century. Petroleos de Venezuela, Caracas, pp. 111–125.
Espitalie, J., Madec, M., Tissot, B., 1980. Role of mineral matrix in kerogen pyrolysis: influence on petroleum generation and migration. American Association of Petroleum Geologists Bulletin 64, 59–66.
Fabuss, B.M., Smith, J.O., Satterfield, C.N., 1964. Thermal cracking of pure saturated compounds. In: McKetta, J.J. (Ed.), Advances in Petroleum Chemistry and Refining. Interscience, New York, pp. 157–201.
Hayes, J.M., 1991. Stability of petroleum. Nature 352, 108–109.
Hill, R.J., Jenden, P.D., Tang, Y.C., Teerman, S., Kaplan, I.R., 1994. The influence of pressure on the pyrolysis of coal. In: Mukhopadhyay, P.K., Dow, W.G. (Ed.), Reevaluation of Vitrinite Reflectance ACS Symposium Series 570.
Hill, R.J., Jenden, P.D., Tang, Y.C., Teerman, S., Kaplan, I.R., 1996. The influence of pressure on the thermal cracking of oil. Energy and Fuels 10, 873–882.
Hill, R.J., Bence, A.E., Behar, F., Curry, D.J., Symington, W. A., Vandenbroucke, M., Lacombre, D., 1999. The effects of retention and secondary cracking on the composition of migratable petroleum. In: 19th International Meeting on Organic Geochemistry, 6–10 September 1999, Istanbul, Turkey, Abstracts Part I, pp. 69–70.
Horsfield, B., Disko, U., Leistner, F., 1989. The micro-scale simulation of maturation: outline of a new technique and its potential applications. Geologische Rundschau 78, 361–374.
Horsfield, B., Schenk, H.J., Mills, N., Welte, D.H., 1992. Closed-system programmed-temperature pyrolysis for simulating the conversion of oil to gas in a deep petroleum reservoir. Organic Geochemistry 19, 191–204.
Huizinga, B.J., Tannenbaum, E., Kaplan, I.R., 1987a. The role of minerals in the thermal alteration of organic matter-III. Generation of bitumen in laboratory experiments. Organic Geochemistry 11, 591–604.
Huizinga, B.J., Tannenbaum, E., Kaplan, I.R., 1987b. The role of minerals in the thermal alteration of organic matter-IV. Generation of n-alkanes, acyclic isoprenoids, and alkenes in laboratory experiments. Geochimica et Cosmochimica Acta 51, 1083–1097.
Ishiwatari, R., Ishiwatari, M., Kaplan, I.R., Rohrback, B.G., 1976. Thermal alteration of young kerogen in relation to petroleum genesis. Nature 264, 347–349.
Ishiwatari, R., Ishiwatari, M., Rohrback, B.G, Kaplan, I.R., 1977. Thermal alteration experiments on organic matter from recent marine sediments in relation to petroleum generation. Geochimica Cosmochimica Acta 41, 815–828.
James, A.T., 1983. Correlation of natural gas by use of carbon isotopic distribution between components. American Association of Petroleum Geologists Bulletin 67, 1176–1191.
James, A.T., 1990. Correlation of reservoired gases using the carbon isotopic composition of wet gas components. American Association of Petroleum Geologists Bulletin 74, 1441–1458.
Jenden, P.D, Newell, K.D., Kaplan, I.R., Watney, W.L., 1988. Composition and stable isotope geochemistry of natural gases from Kansas, Midcontinent, U.S.A. Chemical Geology 71, 117–147.

Jones, D.M., Douglas, A.G., Connan, J., 1988. Hydrous pyrolysis of asphaltenes and polar fractions of biodegraded oils. Organic Geochemistry 13, 981–993.

Kuo, L.-C., Michael, G.E., 1994. A multicomponent oil-cracking kinetics model for modeling preservation and composition reservoired oils. Organic Geochemistry 21, 911–925.

Lewan, M.D., 1985. Evolution of petroleum generation by hydrous pyrolysis experimentation. Philosophic Transactions of the Royal Society of London A 315, 123–134.

Lorant, F., Prinzhofer, A., Behar, F., Huc, A.Y., 1998. Carbon isotopic and molecular constraints on the formation and the expulsion of thermogenic hydrocarbon gases. Chemical Geology 147, 249–264.

Lorant, F., Behar, F., 2002. Late generation of methane from mature kerogens. Energy and Fuels 16, 412–427.

Mango, F.D., 1990. The origin of light cycloalkanes in petroleum. Geochimica et Cosmochimica Acta 54, 23–27.

Mango, F.D., 1997. The light hydrocarbons in petroleum: a critical review. Organic Geochemistry 26, 417–440.

Mango, F.D., 2001. Methane concentrations in natural gas: the genetic implications. Organic Geochemistry 32, 1283–1287.

Mango, F.D., Hightower, J., 1997. The catalytic decomposition of petroleum into natural gas. Geochimica et Cosmochimica Acta 62, 5347–5350.

Mango, F.D., Elrod, L.W., 1998. The carbon isotopic composition of catalytic gas: a comparative analysis with natural gas. Geochimica et Cosmochimica Acta 63, 1097–1106.

McNab, J.G., Smith, P.V., Betts, R.L., 1952. The evolution of petroleum. Geochimica et Cosmochimica Acta 44, 2556–2563.

Pepper, A.S., Dodd, T.A., 1995. Simple kinetic models of petroleum formation. Part II: oil-gas cracking. Marine and Petroleum Geology 12, 321–340.

Price, L.C., 1981. Organic geochemistry of 300 °C, 7 km core samples, South Texas. Chemical Geology 37, 205–214.

Price, L.C., 1995. Origins, characteristics, controls, and economic viabilities of deep-basin gas resources. Chemical Geology 126, 335–349.

Price, L.C., Clayton, J.L., Rumen, L.L., 1979. Organic geochemistry of a 6.9 km deep well, Hinds County, Mississippi. Gulf Coast Association and Geologic Society Transcripts 29, 352–370.

Price, L.C., Clayton, J.L., Rumen, L.L., 1981. Organic geochemistry of the 9.6 km Bertha Rogers #1, Oklahoma. Organic Geochemistry 3, 59–77.

Price, L.C., Schoell, M., 1995. Constraints on the origins of hydrocarbon gas from compositions of gases at their site of origin. Nature 378, 368–371.

Prinzhofer, A., Huc, A.Y., 1995. Genetic and post genetic molecular and isotopic fractionations in natural gases. Chemical Geology 126, 281–290.

Prinzhofer, A., Mello, M.R., da Silva Freitas, L.C., Takaki, T., 2000. New geochemical characterization of natural gas and its use in oil and gas evaluation. In: Mello, M.R., Katz, B.J. (Eds.), Petroleum Systems of South Atlantic Margins: AAPG Memoir, Vol. 73, pp. 107–119.

Rahmani, S., McCaffrey, W., Murray, R.G., 2002. Kinetics of solvent interactions with asphaltenes during coke formation. Energy and Fuels 16, 148–154.

Sassen, R., 1988. Geochemical and carbon isotopic studies of crude oil destruction, bitumen precipitation, and sulfate reduction in the deep Smackover Formation. Organic Geochemistry 12, 351–361.

Schenk, H.J., Di Primo, R., Horsfield, B., 1997. The conversion of oil into gas in petroleum reservoirs. Part 1: Comparative kinetic investigation of gas generation from crude oils of lacustrine, marine and fluviodeltaic origin by programmed-temperature closed-system pyrolysis. Organic Geochemistry 26, 467–481.

Schoell, M., 1995. Episodic migration of natural gas; a new concept of dynamic filling of oil and gas fields. American Association of Petroleum Geologists Bulletin 79, 1247.

Snowdon, L.R., 2001. Natural gas composition in a geological environment and the implications of the process of generation and preservation. Organic Geochemistry 32, 913–931.

Sweeney, J.J., Burnham, A.K., 1990. Evaluation of a simple model of vitrinite reflectance based on chemical kinetics. American Association of Petroleum Geologists Bulletin 74, 1559–1570.

Takach, N.E., Barker, C., Kemp, M.K., 1987. Stability of natural gas in the deep subsurface: thermodynamic calculation of equilibrium compositions. American Association of Petroleum Geologists Bulletin 71, 322–333.

Tang, Y., Perry, J.K., Jenden, P.D., Schoell, M., 2000. Mathematical modeling of stable carbon isotope ratios in natural gases. Geochimica Cosmochimica Acta 64, 2673–2687.

Tannenbaum, E., Kaplan, I.R., 1985. Low-Mr hydrocarbons generated during hydrous and dry pyrolysis of kerogen. Nature 317, 708–709.

Tannenbaum, E.E., Ruth Huizinga, B.J., Kaplan, I.R., 1986. Biological marker distribution in coexisting kerogen, bitumen and asphaltenes in Monterey Formation diatomite, California. Organic Geochemistry 10, 531–536.

Thompson, K., 1983. Classification and thermal history of petroleum based on light hydrocarbons. Geochimica et Cosmochimica Acta 47, 303–317.

Thompson, K., 1987. Fractionated aromatic petroleums and the generation of gas-condensates. Organic Geochemistry 11, 573–590.

Tissot, B.P., Welte, D.H., 1984. Petroleum Formation and Occurrence. Springer-Verlag, New York.

Tsuzuki, N., Takeda, N., Suzuki, M., Yokoi, K., 1999. The kinetic modeling of oil cracking by hydrothermal pyrolysis experiments. International Journal of Coal Geology 39, 227–250.

Ungerer, P., Behar, F., Villalba, M., Heum, O.R., Audibert, A., 1988. Kinetic modelling of oil cracking. Organic Geochemistry 13, 857–868.